THE PENNSYLVANIA STATE UNIVERSITY

UNIVERSITY PARK, PENNSYLVANIA

AFOSR-1910

The Pennsylvania State University

Contract AF 49(638)-504 with Solid State Division,
Air Force Office of Scientific Research, Washington 25, D.C.

Technical Report

Field Emission Studies of Metal Surfaces

Erwin W. Müller
Principal Investigator

December, 1961

Foreword

This report was prepared under contract AF 49(638)-504 at The
Pennsylvania State University, University Park, Pennsylvania, by
E. W. Müller, Research Professor of Physics and project director.
The contract work was started June 1, 1959, and was in part a
continuation of the preceeding contract AF 18(600)-672. The present
research was terminated November 30, 1961. Academic personnel con-
nected at least part-time with this project were Dr. B. C. Banerjee,
Dr. R. D. Young, Dr. M. K. Sinha, and Dr. Y. Yashiro, research
associates, Dr. M. Drechsler, visiting consultant for two weeks,
and Messrs. T. C. Clements, J. F. Mulson, R. Thomsen, and B. J.
Waclawski. The project director wishes to express his appreciation
for the contributions of these coworkers.

ABSTRACTS

Part I.   "Bombardment of Tungsten with 20 Kev Helium Atoms in a
Field Ion Microscope" by M. K. Sinha and E. W. Muller.
Fast helium atoms are shot into the emitter tip of a
field ion microscope, and the resulting damage is shown
to consist of vacancies, interstitials and their clusters.
A large portion of defects created in the interior
appears at the surface. This is due to the high field
stress and the long range of interstitials by focussing
collisions. Mobility of interstitials in tungsten was
observed directly and occurs slowly at $21^{\circ}K$, and fast
at $90^{\circ}K$.

Part II.   "Corrosion of Tungsten by Water and Nitrogen in a
Field Ion Microscope" by J. F. Mulson and E. W. Muller.
Water vapor or nitrogen with a partial pressure of 10^{-6} mm
etch tungsten tips in a f. 'd ion microscope in spite of
the fact that the corroding molecules cannot approach the
depicted tip region directly in the presence of the high
field. The corrosion is a field induced chemical reaction,
and the corrosion species migrate over the tungsten
surface even at liquid hydrogen temperature.

Part III.   "Mass Spectroscopy of the Field Ionization of Hydrogen"
by T. C. Clements, E. W. Muller, and B. J. Waclawski.
H_1^+ and H_2^+ occur in the entire field range from 200 to
500 Mv/cm. H_3^+ was found to be formed in a narrow field
range near best image conditions. Relative H_3^+ production
is independent upon pressure between .5 and 80 microns,
and independent of temperature between $21^{\circ}K$ and $200^{\circ}K$.
Deuterium behaved the same way, and H_2-D_2 mixtures
indicate that the triatomic ion is formed by the direct
reaction of a proton or deutron with a neutral molecule.

Part IV.   "An Improved Method for Electropolishing Fine Tips for
Field Ion Microscopy" by Y. Yashiro and E. W. Muller.
Improved electropolishing is obtained by using pulses
from condensor discharges rather than d.c. Desirable
concave tapers can be made by having the electrolyte
floating in a thin layer on an insulating liquid of
greater density.

Part V.   "Determination of Work Function from Field Evaporation
Data" by E. W. Muller. The formula for field evaporation
contains two unknowns, the field strengths and the work
function. By measuring field evaporation at two different
temperatures two equations are obtained which can be solved
for F and φ. Preliminary measurements indicate the use-
fulness of this new method.

TABLE OF CONTENTS

TABLE OF CONTENTS (Continued)

LIST OF FIGURES

LIST OF FIGURES (Continued)

LIST OF RESEARCH SUBJECTS AND PUBLICATIONS

The results of most of the research performed under contract AF 49(638)-504 have been or are being published in seven papers listed below. The following report will describe additional results that are not contained in these publications. It consists of a compilation of several smaller research projects which have, in our opinion, not yet led to sufficiently definite results to warrant publication in general journals. The investigation of bombardment of tungsten with 20 kev helium atoms was used in partial fulfillment of the requirements for the Ph.D. degree by Mr. M. K. Sinha. The work on corrosion of tungsten by water and nitrogen represents part of a master of science thesis by J. F. Mulson, and some of the study of the mass spectra of field ionized hydrogen was a part of T. C. Clement's master's thesis. Other work to be reported includes an improved method for electropolishing emitter tips, which was tested by Y. Yashiro, and some preliminary considerations of a new method to determine work functions of perfect crystal planes from field evaporation data by E. W. Müller. The following publications are based on work under this contract:

1. E. W. Müller, "Field Ion Microscope Studies of Surface Corrosion, of Interstitials, Vacancies, and α-Irradiation Damage by Controlled Field Evaporation of Atomic

Layers" in "Structure and Properties of Thin
Films", eds. Neugebauer, Newkirk, and Vermilyea,
John Wiley and Sons, pp. 476-489, 1959.

2. E. W. Müller, "Beobachtungen von nahezu fehlerfreien
Metallkristallen und von Punktdefekten im FIM",
Zeit. f. Physik 156, 399-410, 1959.

3. E. W. Müller, "Field Ionization and Field Ion Microscopy", in
"Advances in Electronics and Electron Physics",
ed. Marton, Academic Press, Vol. 13, pp. 83-179,
1960.

4. E. W. Müller, "Observation of Radiation Damage with the FIM" in
"Reactivity of Solids", ed. de Boer, Elsevier
Publ., pp. 682-691, 1960.

5. E. W. Müller and R. D. Young, "Determination of Field Strength
for Field Evaporation and Ionization in the FIM",
J. Appl. Phys. 32, 2425-2428, 1961.

6. R. D. Young and E. W. Müller, "Progress in Field Emission Work
Function Measurements of Atomically Perfect Crystal
Planes", to appear Jan. 1962 in J. Appl. Phys.

7. E. W. Müller, "Direct Observations of Crystal Imperfections by
Field Ion Microscopy", in "Direct Observations of
Imperfections in Crystals", ed. Newkirk, Inter-
science Publ., to appear March 1962.

PART I. BOMBARDMENT OF TUNGSTEN WITH 20 KEV HELIUM ATOMS IN A FIELD ION MICROSCOPE

by M. K. Sinha and E. W. Müller

I. INTRODUCTION

E. P. Wigner recognized in 1942 that the energetic particles such as neutrons and fission fragments in a nuclear reactor, would bombard the solid parts and thereby might give rise to serious technological effects. This lead to theoretical and experimental study of the radiation effects in solids. During the last decade a large amount of experimental work[1] has been done in order to elucidate the nature of the radiation damage in metals, but no generally accepted model has yet been obtained. Most studied metals are copper, silver and gold and the bombarding particles have been neutrons, deuterons, protons, electrons and α-particles. Proton irradiation of tungsten has been studied by E. A. Pearlstein[2] et al and neutron irradiation of W at $77^{\circ}K$ and $300^{\circ}K$ has been investigated by Kinchin and Thompson[3] and at $4^{\circ}K$ and $77^{\circ}K$ by Thompson.[4] In all three cases residual electrical resistivity has been used as an indicator of the damage produced in tungsten.

Generally the nature of radiation damage has been detected by electrical resistivity measurements, tests of mechanical properties, x-ray techniques or by electron microscopy. The changes in the bulk properties of solids have been attributed mainly due to the following atomic defects produced by energetic particle bombardment: (1) vacancies, (2) interstitial atoms and (3) thermal and displacement spikes.

A more direct experimental approach to study the nature of
defects is sought in the present work, by investigating the bom-
barded specimen in a low temperature field ion microscope invented by
Müller.[5] The field ion microscope with a resolution of the order of
atomic separation in metals is naturally the best tool for direct
observation of atomic disorders in a metal. Tungsten tips at liquid
hydrogen temperature have been bombarded by well collimated, about 20
Kev helium atoms and the effects observed. As it is possible to
field evaporate tungsten atoms from the surface of the specimen,
the inside of the material can also be investigated. The temperature
of the tip can be raised and the motion of defects as a result of
low temperature annealing can be observed.

The present study consisted of the following experiments:
a)   specimen bombarded in random crystallographic directions,
b)   specimen bombarded in a direction of close packed atom chains,
c)   field desorption done in order to dig out the damage inside,
d)   specimen tips of different radii bombarded,
e)   tip bombarded at different pressures of helium,
f)   tip bombarded without the high voltage at the tip,
g)   tip was annealed after bombardment in order to study the
     mobility of defects at different temperatures,
h)   tip bombarded by much heavier atoms of mercury.

The intensity of the helium atom beam hitting the specimen tip
has been measured and the number of hits per second on the tip calcu-
lated. The number of displaced atoms have been calculated and com-
pared with the experimental value.

The important limitation of the present investigation is that the surface of the material is under a large outward stress due to the high electric field. Although the tip can be bombarded with the field off when it is free from stress, it is not possible to see the image of the surface without this stress.

II. EXPERIMENTAL

Apparatus

The main experimental tube designed for studying the effect due to bombardment of tungsten emitter with helium atoms is shown in Fig. 1. It consists of two parts, the conventional low temperature field ion microscope and a Penning discharge tube with accelerating electrodes for producing the bombarding beam. The field ion microscope has been described in detail elsewhere in literature.[6] In a typical design the specimen tip is supported on tungsten leads which are sealed in the bottom of a cold finger inside the microscope tube. The cold finger has a conical ground part which is enclosed by a copper or aluminum sheet cone in order to cool the tip environment. This increases the intensity of the image due to increase of the number of gas molecules arriving at the tip. In the present experiments the cone has a slit at the level of the tip for the particle beam to pass through and hit the tip. The lower part of the microscope tube including the side walls and the screen base has a conductive coating of transparent tin oxide, which together with the metal cone is kept at ground potential, while the tip is connected to positive high voltage.

Fig. 1

HIGH VOLTAGE +

LIQUID HYDROGEN

CONDUCTIVE COATING

SCREEN

TO PUMP

≡ +20 K·V·

900v

H

LIQUID NITROGEN
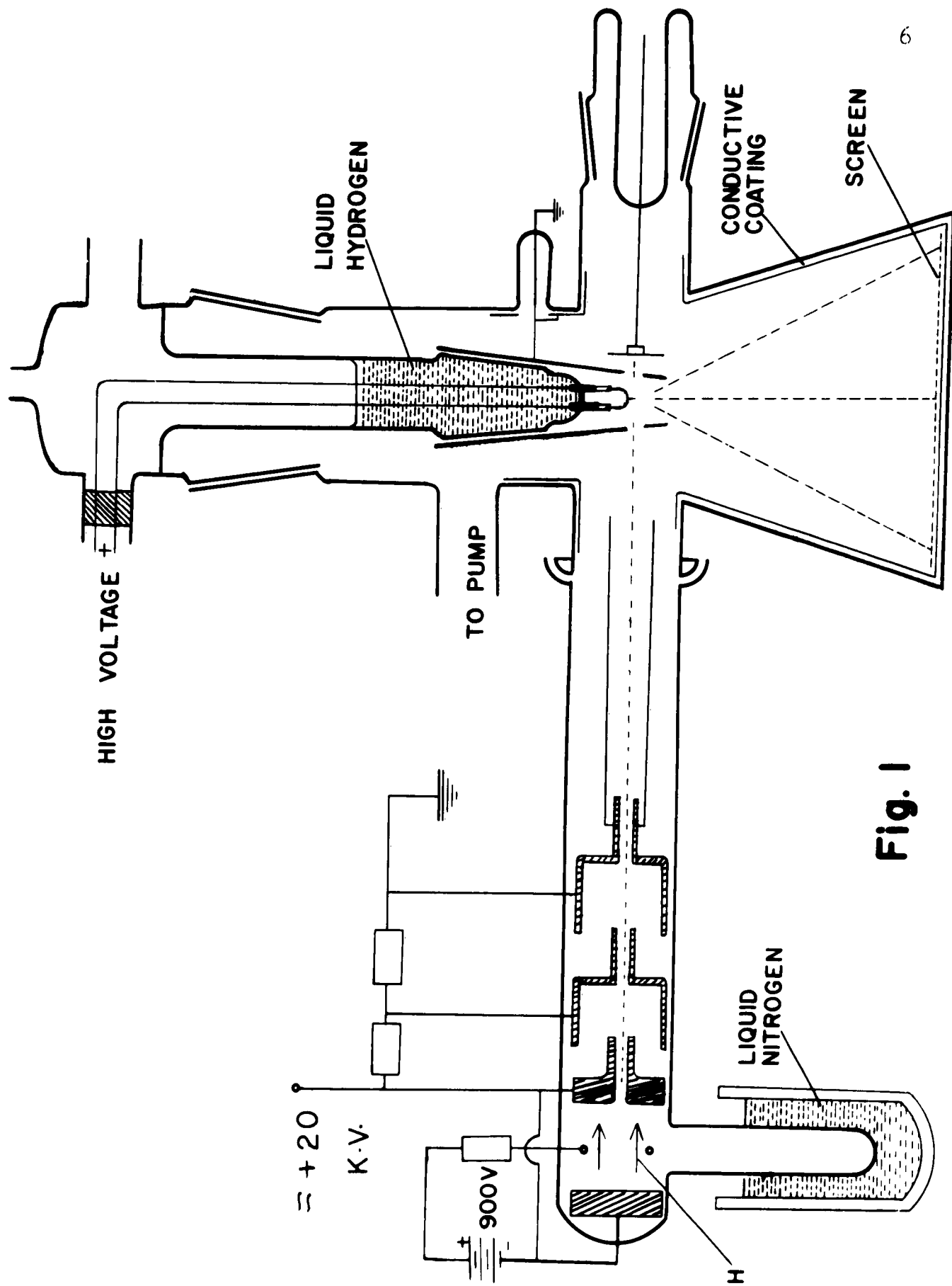
The modifications in the microscope design used in the present work are two side arms. One arm connects the microscope, through a ground ball joint, to the tube having the Penning discharge and accelerating electrodes. The other arm is for holding a fluorescent screen to see the shadow of the tip in the beam while it is being bombarded, or a Faraday cage when the helium ion beam current is measured. This arm can also be used for holding a getter when better vacuum conditions are required.

The Penning discharge consists of two cylindrical cathodes and a ring anode placed between them. The cathodes are of iron, each 3.5 cm long and 2.5 cm in diameter and are sealed in a glass tube 2.5 cm apart. The anode, a tungsten ring of 1.5 cm diameter is placed between the cathodes. One of the cathodes has a hole of about 2 mm diameter to pass the ion beam through it. An axial magnetic field is applied between the electrodes by a permanent magnet. A potential difference of 900 volts between the electrodes is sufficient to ignite the discharge down to 1 micron of helium. Pressures of about 1 to 4.5 micron of helium have been used in the experiments. These limits are necessitated because the microscope and the Penning discharge are at the same pressure. At low pressures, the intensity of the image decreases so much as to make visual observation difficult and requires long exposure times for photographing the image. On the other hand, if the pressure is increased, the intensity increases but the image becomes blurred resulting in loss of resolution. This is caused by the scattering of helium ions, on their way to the screen, by the gas molecules. The range 1 to 4.5 microns is suitable in order to have good image intensity without much loss of image quality.

The accelerating electrodes acting as coaxial cylindrical ion lenses are made of stainless steel and are kept at such voltages so as to focus the ion beam on the specimen tip. With the help of a micrometer arrangement, the Penning discharge tube can be moved horizontally and vertically in order to direct the ion beam exactly on the tip. This can be seen on the fluorescent screen held in the other side arm. Just below the Penning discharge is a liquid nitrogen trap which condenses out most of the impurities present in the discharge such as mercury, hydrocarbons and sputtered contaminations from the electrodes

The vacuum system is a conventional one including a 35 mm orifice two stage mercury diffusion pump with a mechanical pump. A Mcleod gauge connected to the microscope measures the pressure and there are two liquid nitrogen traps in series placed between the diffusion pump and the experimental tube. A steel ball cut-off valve is employed to let a measured amount of helium gas in the microscope through the Mcleod gauge. This valve consists of a precision ball bearing steel sphere of 3/8 inch diameter resting in the closed position on a finely ground seat. It can be operated from outside by a magnet.

The high voltage source used for operating the microscope is a 0-30 kv dc power supply model 230-5 manufactured by the Beta Electric Corporation, and that for accelerating ions is a 0-30 kv power supply made by the Potter Company. The 900 volt battery for the Penning discharge consisted of three, 300 volt dry batteries. The high voltage measurements were made with an electrostatic voltmeter, 0-30 kilovolts, Model ESH of Sensitive Research Company.

The potential divider for focussing the ion beam on the tip
is made of a number of amply dimensioned BFQ, BFW resistors of
Resistor Products Company.

An F:1 objective camera is used for photographing the images
because of their low intensity, except when the radius of the tip
is quite large and the intensity high enough to permit F:2 aperture.
The film used is Kodak spectroscopic film type 103-A-G and is
processed with the highly active ethol developer. The exposure time
varies with the radius of the tip and the pressure of helium.
Typical exposure times for the present experiments were from about
20 seconds to one minute and thirty seconds.

The Experiments and their Results

1. Measurement of helium ion beam current.

To compare results with the theoretical ones it is necessary
to know the number of bombarding particles hitting the specimen tip
in a given time. With the tip at high voltage of 10-20 kv, it will
be bombarded mostly by the neutral helium atoms which are formed in
the ion beam as a result of charge changing collisions. Their
number can be estimated by measuring the ion current and using the
known value[7] of charge changing cross-section of He^+ to He in helium
gas.

The bombarding ion beam current was measured by using a
Faraday cage as the ion collector. It was designed in such
a way as to eliminate the secondary electron current. The
front face of the outer cylinder has a fluorescent screen on it to
observe the ion beam. The currents were measured with a Keithley
electrometer model 210 using a decade shunt, model 2008. Helium

gas at known pressure was admitted in the tube and the Penning discharge ignited. The ion beam was accelerated and entered the Faraday cage. The beam current was measured with the outer cylinder kept at voltages from +90 to -90 volts. The results for various pressures are shown in Figs. 2 a, b, and c. When the outer cylinder is kept at increasing positive voltages, the current increases rapidly and seems to approach a saturation value. This is to be expected as the secondary electrons from the cage are attracted to the outer cylinder. With the outer cylinder at negative voltages the current first decreases rapidly up to -10 v and then decreases very slowly showing that most of the secondary electrons are of rather small energy. The very slow decrease is probably due to the secondary positive ions released from the Faraday cage by the impact of the ion beam. The value of current with the outer cylinder at -20 v was taken to be the ion current. Table I gives the ion beam current at various pressures. It also gives the corresponding Penning discharge current. The circuit of the discharge had a 940 k Ω external resistance.

2. Measurement of the cross section of beam.

In addition to the measurement of ion beam current, the cross section of the beam is to be known for calculating the number of particles striking the specimen tip. This was done as follows: the ion beam was focussed on one side of the hole in the outer cylinder of the Faraday cage, with the help of the micrometer arrangement for moving the Penning discharge tube. The current as registered by the cage was measured. Then the screw was rotated by one turn and the current again noted. This was done till the beam
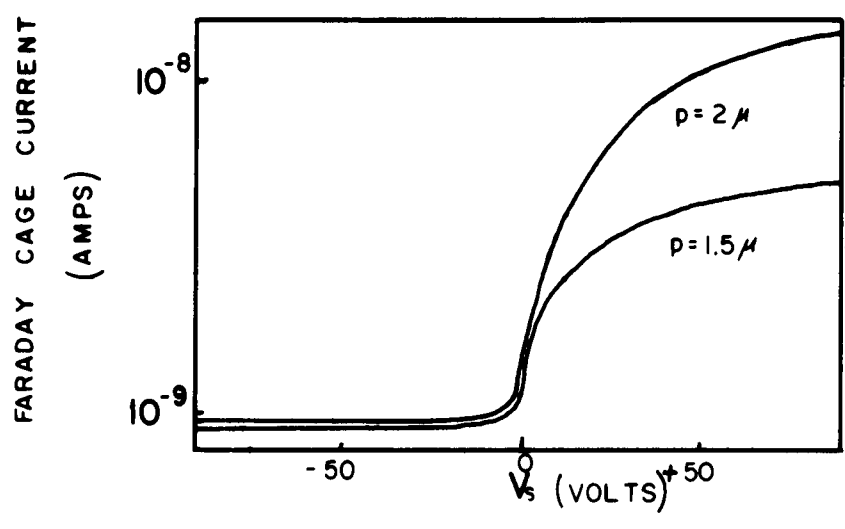
Fig. 2a
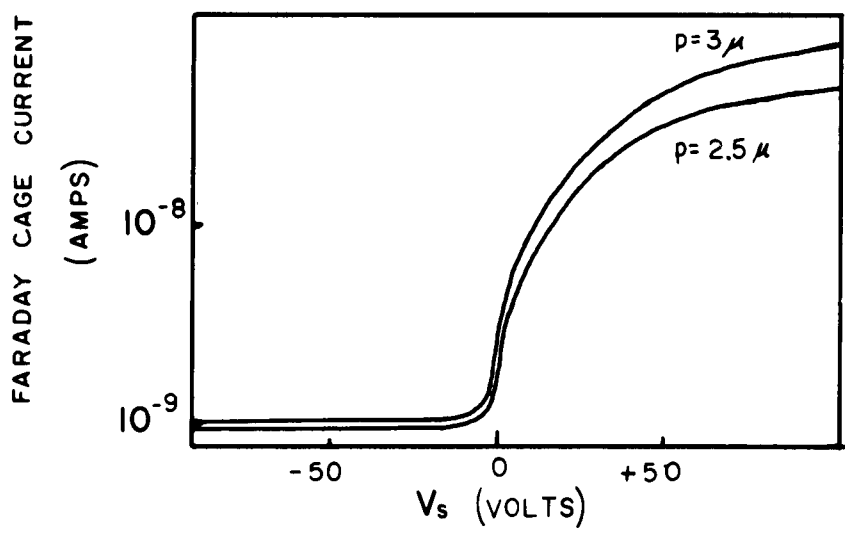
Fig. 2b
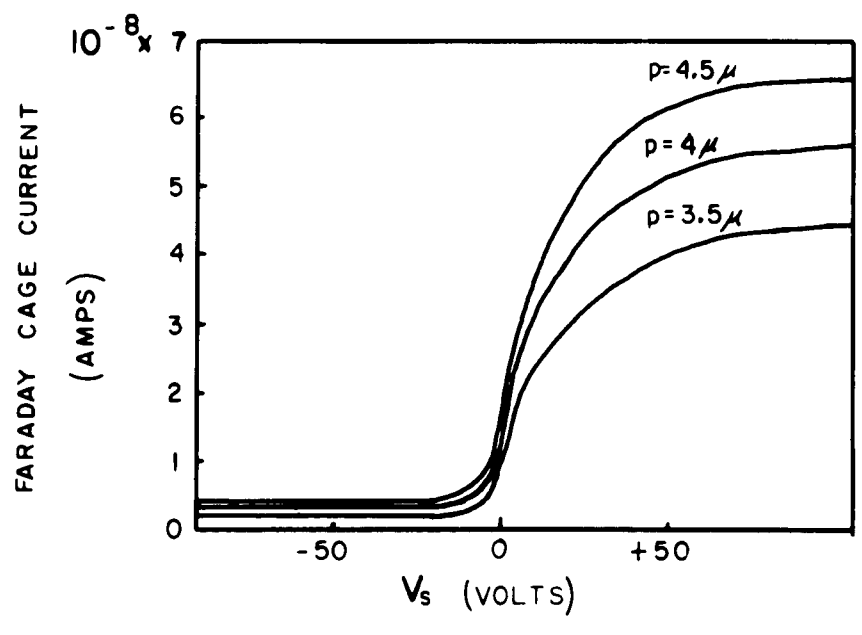
Fig. 2c

TABLE I

Ion beam current at various pressures
with the outer cylinder at -20 volt.

Pressure (microns)	Current (amps)	Penning dis- charge current (microamps)
1.5	7.7 x 10^{-10}	17
2	8.8 x 10^{-10}	30
2.5	9.5 x 10^{-10}	40
3	1.15 x 10^{-9}	55
3.5	2.3 x 10^{-9}	64
4	3.3 x 10^{-9}	80
4.5	4.8 x 10^{-9}	91

spot passed by the hole and was on the other side of it. This

can be seen on the fluorescent screen made on the face having the

hole. The Fig. 3 shows the variation of cage current as the beam

spot passes from one side of the hole to the other side. It is

to be noted in Fig. 3 that the curve is not symmetric as might be

expected. The reason is the way in which the Faraday cage and the

fluorescent screen with the hole was mounted in the side arm. The

screen was purposely kept in a slanting position as shown in Fig. 4,

in order to view easily from outside the beam and the shadow of

the tip on it. It is clear from the figure that the beam passes a

sharp edge on one side of the hole while more diffuse scattering is

expected on the other side. The greater slope in the curve

corresponds to the sharp edge. Because the hole is circular it is

estimated that when the center of the beam lies on the edge of the

FARADAY CAGE CURRENT AMPS

SCREW ROTATIONS

Fig. 3

ION BEAM

SCREEN   FARADAY CAGE
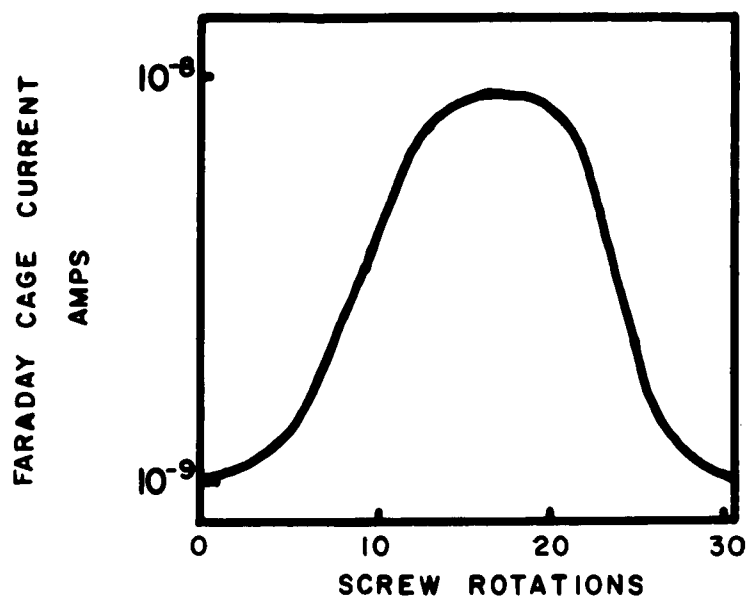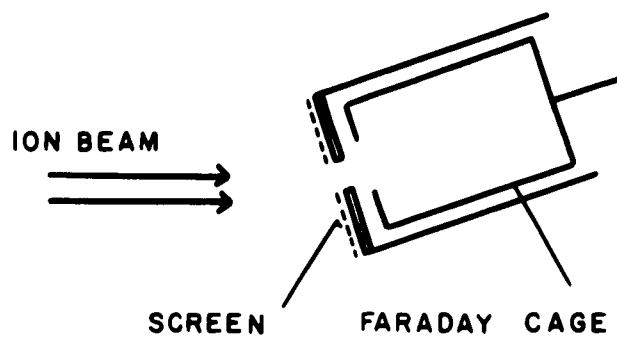
Fig. 4

DERIVATIVE OF THE CURVE IN FIG. 4

SCREW ROTATIONS
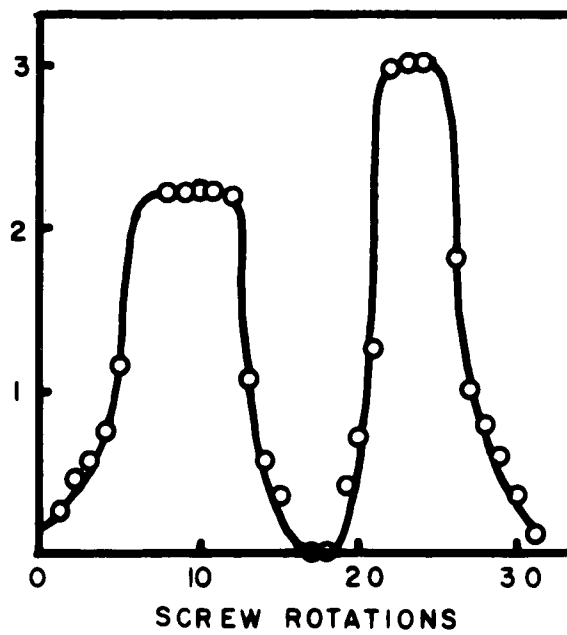
Fig. 5

hole, about 40% of the total current enters the Faraday cage. Thus
the distance between the points of the curve corresponding to 40%
of the total current gives the diameter of the hole in terms of
number of turns of the screw. Knowing the diameter of the hole,
the screw is calibrated. Figure 5 is a plot of the numerical
derivatives at various points of the curve in the Fig. 3. For
determining the width of the beam the points midway between the
maximum and minimum values of the derivatives on the steeper
side of the curve in the Fig. 3 were taken. The width of the
beam measured in this way was 1.3 mm.

3. Estimation of the number of particle hits on the tip.

The number of neutral atoms in the ion beam is calculated by
using the equation

$$N(\ell) = N_0 \, e^{-n\sigma_{10}\ell}$$

where $N(\ell)$ = number of ions after traveling distance ℓ in the
gas having n atoms per unit volume

N_0 = number of ions initially

σ_{10} = charge changing cross-section per atom from He^+
to He in He gas.

The value of σ_{10} for 20 kev He ions is taken from reference 7
and is equal to 5.2×10^{-16} cm^2 per atom. In our experiments
the distance traveled by the ions between the last lens and the
tip was 20 cm. Table II gives the calculated values of the
fractions of neutral atoms at various pressures. The ion
current having already been measured, the number of neutrals in the
beam is found. The area of the tip exposed to the beam is taken equal

THIS
PAGE
IS
MISSING
IN
ORIGINAL
DOCUMENT

TABLE II

Percentage of neutral atoms in 20 kev He$^+$ beam
in He gas after traversing 20 cm of gas.

Pressure (microns)	Neutral atoms in %
1	29
1.5	40
2	49
2.5	57
3	64
3.5	69
4	74
4.5	78

to 1.25 r^2, where r is the radius of the tip. Generally the clear
portion of the ion picture is that bounded by the two {111} planes
with the plane (011) in the centre. The angle between (011) and
(111) planes is 35°16' and hence the area of the tip facing the
beam is approximately 1.25 r^2. The radius of a tip is determined in
the following way:[8] The ion image of a tip is its perfect
topographic map with the lattice steps as contours. The Fig. (6)
gives the orthographic projection of a tungsten crystal with (011)
plane in the centre. The number n of net plane rings of known
step height h between a certain apex angle is counted and this gives
the height of the cap n$_t$h. If this apex angle is θ, the local radius
of curvature of the tip is then given by

$$r = \frac{nh}{1-\cos \theta} .$$
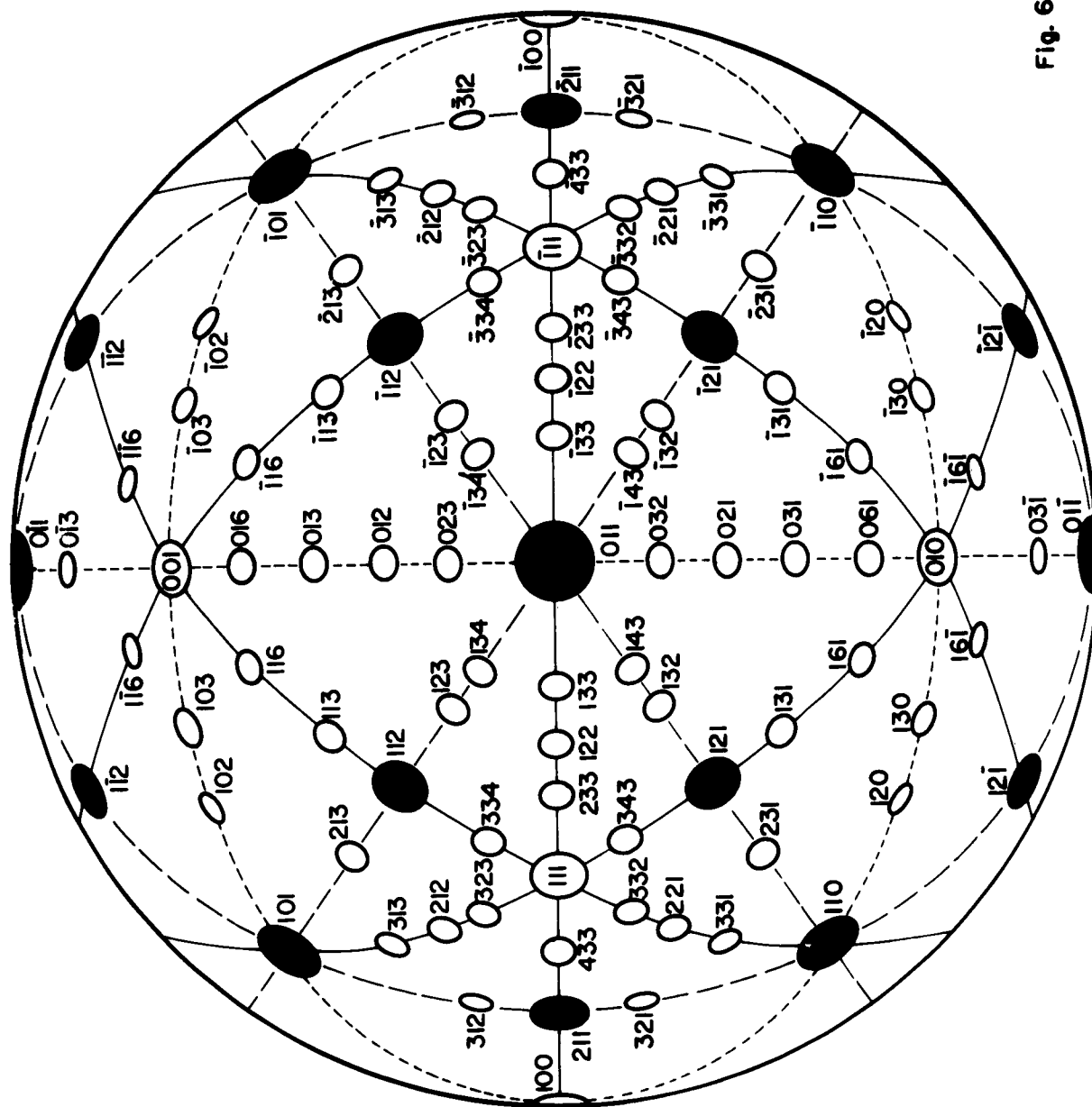
Fig. 6

The angle θ between the normals of two net planes with Miller indices $(h_1k_1\ell_1)$ and $(h_2k_2\ell_2)$ is calculated by

$$\cos\theta = \frac{h_1h_2 + k_1k_2 + \ell_1\ell_2}{\sqrt{h_1{}^2 + k_1{}^2 + \ell_1{}^2}\sqrt{h_2{}^2 + k_2{}^2 + \ell_2{}^2}}$$

The net plane rings used in the present experiments are those of (011) plane with step height of 2.24 $\overset{o}{A}$ and the apex angle is that between (011) and (123) or (112) planes. The calculated values of the number of hits per second of neutral atoms on the tip at various pressures are given in Table III.

TABLE III

Number of hits/second on a tip of 500 $\overset{o}{A}$ radius at various pressures.

Pressure (microns)	hits/sec.
1.5	1
2	1.7
2.5	2.4
3	4
3.5	10
4	18
4.5	33

4. Bombardment of specimen tips.

In all experiments performed the helium gas used was obtained from Linde Products Company and the tungsten wire used for specimen tips was General Electric 218 NS-wire, annealed, 0.004" thick. The

fine tips were made by electrochemical etching of the wire in molten $NaNO_2$ with a few volts ac. The progress of the etching is checked by observing in an optical microscope. Although the actual end of the tip with radius from 300 $\overset{o}{A}$ to 1000 $\overset{o}{A}$ cannot be seen with optical means, but with experience one can tell if the tip has a promising cone shape. After the tip was inserted in the ion microscope tube and good vacuum obtained, they were always annealed to dull red heat for a few seconds before the actual experiments. This heating cleans the tips and allows recovery of residual strain by eliminating mobile dislocations. While bombarding, the tips are at about 21^oK as the cold finger through which the high potential leads pass, is filled with liquid hydrogen.

The technique for operating a field ion microscope is given in detail elsewhere.[6] First the Penning discharge and microscope tube is evacuated to about 10^{-6} mm of Hg pressure, then cut off from the pumps and a known amount of helium gas is let in and ion image obtained by applying positive high voltage at the tip. One might think that with an ititial vacuum of 10^{-6} Torr. and ground joints with grease, there would be enough impurity gases in the tube to contaminate the tip surface with at least a monolayer within seconds. The great advantage of the helium ion microscope is that these apparently poor vacuum conditions do not affect its operation. The fact that the cold finger is filled with liquid hydrogen throughout the duration of the experiments causes the system to act like a dynamic one as the vapour pressure of contamination gases like O_2, N_2 is of the order of 10^{-10} Torr at 21^oK. Further, as the specimen is at an electric field of about 500 MV/cm while under observation,

no contamination gases can reach it. All such gases that may occur in the vacuum system have ionization energies near or below 15 ev, while helium with 24.47 ev has the highest ionization energy of all elements. The contamination gases are ionized at a field of about 200 MV/cm which is at a distance of about twice the radius of the tip above it, and are carried away towards the screen producing a weak background light. The specimen surface, therefore, remains clean so long as the high voltage is on. Because of this reason most of the bombarding experiments were done with the tip at high voltage.

When the helium atom beam is directed onto the specimen, the tip shadow is seen on the fluorescent screen which is held through the sidearm opposite to the Penning discharge tube. Thus the beam can be accurately focussed on the tip. Besides the helium atoms striking the tip, there might be some impurity atoms present in the beam as a result of the sputtering of the metal electrodes and the residual gases in the electrodes and the apparatus. Although the number of impurity positive ions due to sputtering (only positive ion will be accelerated towards the tip) should be extremely small[9] so as not to cause any appreciable damage to the specimen, precaution is taken to focus only the helium beam on the tip. This is done by deflecting the ion beam by an electromagnet placed around the glass tube and after the ion lenses. The tip is bombarded for the required time and the photograph of the image taken.

The changes occurring on the surface of the specimen as a result of bombardment or annealing are detected by comparing the two photographs taken before and after such occurrence. This is done

by viewing simultaneously the first picture through a red filter and the second through a green filter with the help of a beam splitter.[10] When the two images are in coincidence the common parts of the two pictures appear yellow while the new atoms in the second photograph appear green and those atoms that are removed from the first and are not in the second look red. This colored picture can also be photographed. However, for economical reasons these color photographs are not included in this report.

5. Theoretical considerations.

The moving helium atoms will produce displacement of stationary tungsten atoms by elastic collisions, interacting with one atom at a time. Following Bohr,[11] it can be assumed that in such collisions the atoms interact with a screened coulomb potential energy, of the form

$$V(r) = \frac{Z_1 Z_2 e^2}{r} e^{-r/a} \tag{1}$$

where Z_1, Z_2 are the atomic numbers of the two particles, r is the separation of the two atoms and a is the screening constant. The screening constant is given by the approximate relation

$$a = \frac{a_0}{(Z_1{}^{2/3} + Z_2{}^{2/3})^{1/2}} \tag{2}$$

where a_0 is the Bohr radius of hydrogen ($a_0 = 5.29 \times 10^{-9}$ cm). Whether the collision can be considered a hard sphere type or Rutherford type is governed by a parameter b, the closest distance of approach of the two nuclei in the absence of screening and is given by

$$b = \frac{2E_1 Z_2 e^2}{\mu V^2}$$

where μ is the reduced mass of the two particles and V is the velocity of the incident particle. If b $\overline{>}$ a, one can assume the collisions to be of hard sphere type and if b $\ll$ a, Rutherford theory can be applied. The above criterian gives a critical energy E_c, given by

$$E_c = 2E_R \left[\frac{M_1 + M_2}{M_2} \right] Z_1 Z_2 \sqrt{Z_1^{2/3} + E_2^{2/3}} \qquad (3)$$

where E_R (= 13.6 ev) is the Rydberg energy, such that if the energy of the moving particle $E \gg E_c$, the collisions are of Rutherford type and if $E \overline{<} E_c$, the collision can be considered of hard sphere type. The value of E_c for He and W atoms is about 18 kev. In our experiments the energy of helium atoms being about 20 kev, the calculations are based on hard sphere theory, but the results that are obtained on the other extreme approximation of Rutherford collisions will also be considered.

In hard sphere collisions, the differential cross-section for energy transfer from T to T + dT is given by

$$d\sigma = cdT \qquad (4)$$

where

$$C = \frac{\pi R^2}{T_m}.$$

Here R is the radius of the effective hard sphere, approximately equal to the screening constant given by (2) and T_m is the maximum energy transfer in such a collision, given by

$$T_m = \frac{4M_1 M_2}{(M_1 + M_2)^2} E \qquad (5)$$

In order to find the total cross-section for a collision in which the target atom is displaced from its lattice site, one usually

takes the lower limit of T in (4) as T_d, the threshold energy to displace an atom. The atoms are assumed to be bound in a simple square-well potential of height T_d. Thus, the total displacement cross-section is given by

$$\sigma_d = \int_{T=T_d}^{T=T_m} c \, dT = \pi R^2 \left(\frac{T_m - T_d}{T_m} \right). \tag{6}$$

The mean free path L for displacement collisions is found by

$$L = \frac{1}{n_o \sigma_d} \tag{7}$$

where n_o = number of atoms per unit volume in the target material.

In Rutherford collisions, one can show that the total displacement cross-section is given by

$$\sigma_d = c' \left(\frac{1}{T_d} - \frac{1}{T_m} \right) \tag{8}$$

where $c' = \pi Z_1^2 Z_2^2 e^4 \left(\frac{M_1}{M_2} \right) \frac{1}{E}$ and $Z_1 e$, $Z_2 e$ are the charges of the two nuclei.

6. Bombardment of tips in random crystallographic direction.

When specimen tips have been bombarded by He atoms in random crystallographic direction, three types of damage has been observed. These are vacancies, interstitial atoms or their clusters and a disordering of atoms in a region of 50 - 100 $\overset{o}{A}$ diameter. The Figs. 7, 8, 9 and 10 show the different types of damage produced and seen on the surface of the tip. The vacancies and interstitials are seen on both sides of tip, the entrance side of the beam and the exit side, although their number is, in general, not the same on the two sides. The clusters of interstitials or general disordering is also found on both sides. The interstitials appear
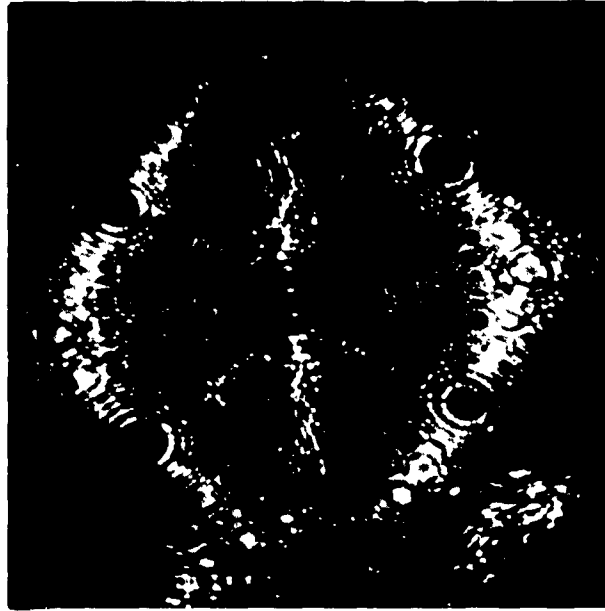
Fig. 7a

Fig. 7b

Fig. 8a

Fig. 8a
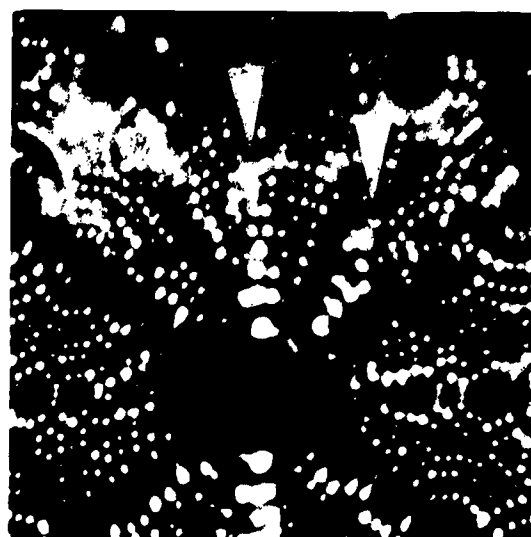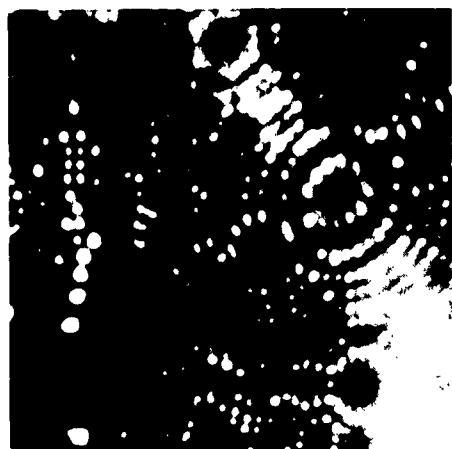
Fig. 9a
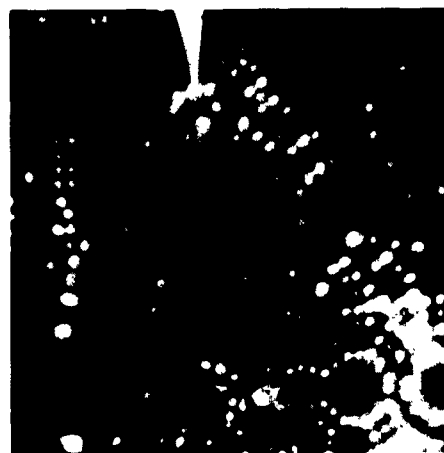
Fig. 9b

Fig. 9c
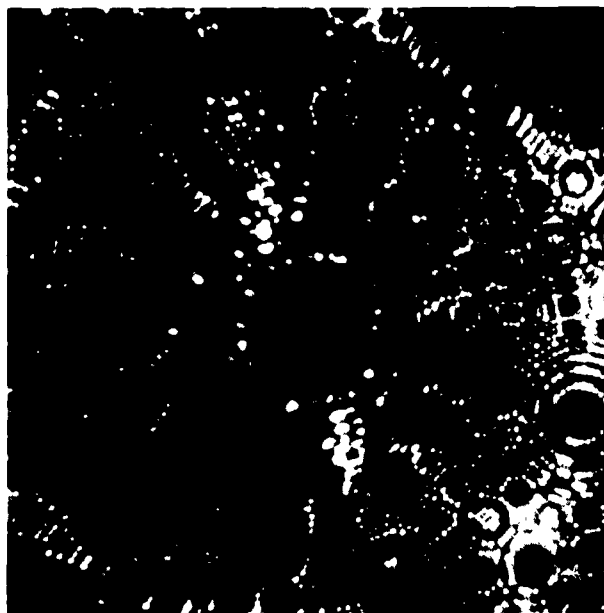
Fig. 10 a
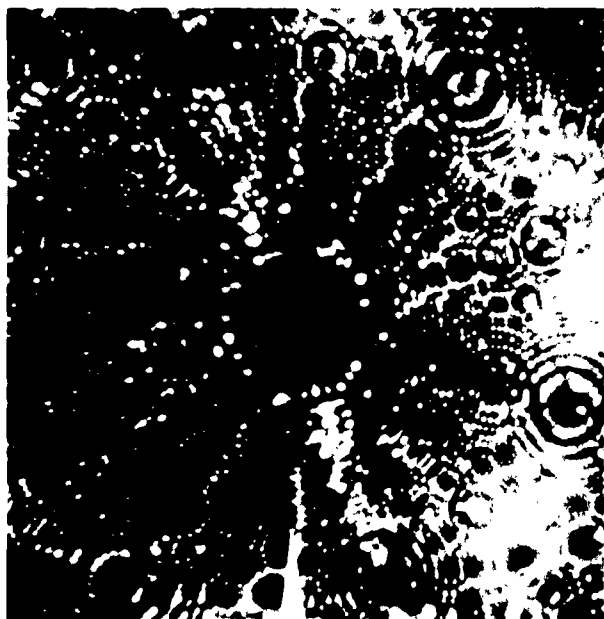
Fig. 10 b

as bright points on the screen, and in different diameters, depending upon their exact position on top of a net plane or within the top layer, where they bulge out the surface over a wide area.

Figure 7 is the image of a tip about 650 A radius and shows a cluster and a few interstitials as a result of bombardment. The cluster on the exit side is seen near the $(\bar{1}32)$ plane. On the entrance side there are two interstitials, one near the (143) plane and the other near (132) plane. It might be that the helium atom entered the tip somewhere between the above two planes producing the two primary knock-ons and the cluster on the other side may be the secondary knock-ons produced by a displaced W atom.

Figure 8 shows a tip of about 400 A radius. The Fig. 8(a) is a photograph of an unbombarded tip and the Fig. 8(b) shows the same tip after bombardment. Two clusters are seen on the entrance side, one on (012) plane and the other near the $(\bar{1}23)$ plane.

Figure 9(a) shows a 350 A radius tip. When bombarded, besides some interstitials and vacancies, a region of about 50 A radius near the (131) plane is damaged (Fig. 9(b)). This region appears to have a small 'pit' in the center with a disordering around it. Such a damage might be due to the production of a thermal spike as suggested by Seitz.[2] The average energy of a primary knock-on in the present case will be about 800 ev and it can produce such a spike. The region of damage in such a case will be the intersection of the thermal spike with the surface of the tip. The atoms in the center should be field evaporated and there should be disordering around this spot. Figure 7(b) perhaps shows such a case. The Fig. 9(c) shows the result of further bombardment. The (121) plane

is particularly damaged, with one atom ring of the plane incomplete. The atoms seem to be displaced towards the right side and the region is rather disturbed.

Figure 10 shows a tip of about 550 A radius and here the interstitials produced are very clearly seen on the (011) plane in Fig. 10(b). The picture before the bombardment, Fig. 10(a), was obtained after the field evaporation of a bombarded tip. It shows four atoms on the (011) plane. When the tip was further bombarded, 15 more displaced atoms appear on the (011) plane. That such interstitials are definitely the result of bombardment, is supported by the fact that if the tip is not bombarded and the ion image is allowed to stay on the screen, there is not a single change found on the surface of the tip even after a few hours. In these bombardment experiments the next picture is generally taken only after some seconds.

The fact that layer after layer of tungsten atoms can be removed by field evaporation makes it, in principle, possible to see the damage inside the tip. But tungsten does not seem to be a good material for such observations. Several factors caused such experiments to be unsuccessful.

The field evaporation can be controlled best when the difference between best image field and evaporation field is small, for then one can clearly observe the surface of the tip as the evaporation proceeds. In tungsten, the evaporation field at $21^{\circ}K$, being about 20% greater than the best image field, the image no longer remains distinct when evaporation is performed. Platinum

would be a very good material for such observation for in its case the field evaporation takes place at almost best image field.

Another difficulty is that as the field is increased at the tip, gradually the interstitials are seen to leave the surface as a result of increase of the surface stress; and by the time of evaporation field, all of them leave. Hence as evaporation proceeds, most defects will probably not stay on the surface and unless simultaneous distinct observation is possible, they probably cannot be seen. Vacancies produced in the interior by bombardment should be visible in this way, but to make sure that these are due to bombardment, one should have a perfect single crystal tip to start with and this was not the case in the present experiments.

7. Bombardment of tips in close packed direction.

Experiments have been done, in which the tip was bombarded in the close packed direction in order to see if the damage depends on the direction in which the particle beam strikes the tip. In one experiment the tip was bombarded in a direction in which the atoms are not close packed, while in another one it was bombarded in a direction of close packed atom chains. Both the tips were of about the same radius (450-500 A) and both were bombarded for one minute at 3 microns of helium. These experiments indicate that the amount of damage increases when the tip is bombarded in the close packed direction. For example, in the first case above the total number of interstitials are about 140 and in the second one they are about 55. There does not appear to be any difference in the ratio of damage on the exit and entrance side; it being 1.8 in both cases.

8. Bombardment of tips of different radii.

The mean free path of those collisions which produce displace-
ment of a tungsten atom is given by Eq. (7) of Sec. 5. It gives
L = 170 A for $^{\beta}$ therford collisions and 360 A for the hard sphere
approximation. If the tips of different radii are bombarded, it is
to be expected that the damage on the two sides of a tip should
depend on its radius. Table IV gives the ratio of damage on the
two sides of tips of different radii, when they were bombarded
for five seconds.

These observations can be explained in the following way.
When the radius of the tip is smaller, say 200 - 300 A, because of
the scattering of helium atoms at random directions in the tip
there will not be much difference in displacements of the tungsten
atoms on the two sides. On the other hand if the radius is large
compared to the mean free path for displacement collisions, more
displacement can be expected on the entrance side including the
central part of the tip.

TABLE IV

Ratio of displaced atoms on the entrance side
and exit side of the tip of different radii.

Radius of tip (A)	Ratio $\dfrac{\text{displaced atoms ent. side}}{\text{displaced atoms exit side}}$
200	1
300	1.8
400	2.3
550	3.3
900	5

9. Bombardment of tips at different pressures of helium.

If the pressure of helium in the microscope and Penning discharge tube is varied the number of helium atoms striking the tip will vary and so will the damage to the tip. The number of primary knock-ons, n_p, produced per unit volume of the specimen is given by

$$n_p = \varphi \, t \, n_o \, \sigma_d \qquad (9)$$

where φ = number of particles traversing unit area per unit time in the specimen, t = time of bombardment, n_o = number of atoms per unit volume of the specimen, σ_d = displacement cross-section. To find the total number of displaced atoms, the number of secondaries per primary are to be calculated. One can show that the number of atoms displaced per primary knock-on is given by[1(b)]

$$n_s = \frac{\bar{E}}{2 \, T_d} \qquad (10)$$

where $\bar{E}$ is the average energy of the primary knock-on. Combining Eqs. (9) and (10), the total number of displaced atoms per unit volume will be given by

$$N_d = n_p \cdot n_s \qquad (11)$$

Specimen tips were bombarded with pressures from 1.5 to 4.5 microns and the Table V gives the displaced atoms counted on the surface of the tip and calculated in the volume of the tip from Eq. (11). The bombarding time in each case is five seconds.

In calculating the number of displaced atoms, the flux 0 is taken as the number of particles hitting that part of the tip which is shown on the screen and faces the beam. Actually, those particles which hit the shank of the tip and which is not visible on the screen may also produce some displaced atoms in the visible region. Likewise,

TABLE V

Number of displaced atoms in $(t = 5")$.

Pressure (Microns)	Counted on the surface	Calculated in the volume of the tip
1.5	4	15
1.8	5	25 (at 2 microns)
2.5	22	31
3	44	62
3.5	52	145
4	60	260
4.5	110	480

the particles hitting the visible portion may displace atoms in the region of the shank.

Further, the value of the threshold energy for displacement of W atoms has neither been determined experimentally nor calculated theoretically. It has been usual to assume the value of T_d to be equal to 25 ev for all metals. But some recent investigations show that this might be in much error. Walker[13] reports that in the noble metals the threshold energy increases with increasing atomic number and in Au may be as high as 40 ev. In Cu, for which T_d has been generally taken as 25 ev, very different results for different crystallographic directions have been recently found by Gibson[14] et al. In the absence of any known value for W, it seems reasonable to assume an average value of 25 ev for T_d. In the calculations this value has been used.

In an ion microscope, one can see only about one atomic layer deep, still the damage seen is a quite high fraction of that calculated. The surface of the tip acts as a sink for the defects, hence they can migrate to it. Further, the value of T_d may be in error.

10. Bombardment of tips with Hg atoms.

To compare the damage produced by helium atoms with that produced by much heavier particles some experiments have been done in which the tip is bombarded by Hg atoms or ions. In order to get mercury atoms in the beam hitting the tip, some Hg is condensed in the liquid nitrogen trap below the Penning discharge. This is done by putting liquid nitrogen around this trap after good vacuum is obtained in the system but the two liquid nitrogen traps after the mercury diffusion pump are not in liquid nitrogen. Thus, the mercury vapors in the tube condense in the trap below the Penning discharge. Then, the traps after the diffusion pump are also put in liquid nitrogen. As usual, helium is let in the microscope and the ion image obtained. When the tip is to be bombarded by Hg atoms, liquid nitrogen is removed from the trap under the Penning discharge. The trap gradually warms up and the discharge contains Hg vapor as can be seen by the change of the color of discharge. If now the beam is focussed on the tip it will be hit by some Hg atoms. As soon as the beam is directed on the tip the effect of bombardment is clearly seen in the image. The damage to the tip is much different and more spectacular. Essentially two types of damage occur: first, a large number of clusters or complete

disordering occurs on all parts of the image, and second, actual field evaporation of the (011) planes takes place. This is to be expected as Hg atoms with much heavier mass than helium impart much more energy to W atoms. The field evaporation of (011) planes can be explained in the following way. The desorption energy Q_0 of metal ion from its surface is given by

$$Q_0 = \triangle + V_1 - \varphi$$

where $\triangle$ = energy of vaporization, V_1 = ionization energy, and φ = work function of the metal. Q_0 is derived from the thermionic cycle by considering first the evaporation of a neutral atom, then its ionization and finally putting the electron back into the metal. In the presence of an electric field as is the case in the ion microscope, the energy barrier Q which has to be overcome in order to field evaporate is reduced from Q_0 by the effect of the field and is given by

$$Q = Q_0 - \sqrt{e_3F} \ .$$

The value of Q for tungsten, taking F equal to 450 MV/cm and known values of $\triangle$, V_1 and φ ($\triangle$ = 8.67 ev, V_1 = 7.98 ev, φ = 5.99 ev) is found to be 2.4 ev. The average energy imparted by a Hg atom to W atom in a collision will be about 10 kev. If we consider that the radius of the (011) plane evaporated is 100 A, then it contains about 5000 atoms and they will need about 12 kev to field evaporate. Thus a possible explanation is that the Hg atoms impart most of their energy to tungsten atoms near the surface of the tip. Figure 11(a) and (b) shows the bombardment of a tip by Hg atoms. In addition to a number of interstitials and vacancies, there are several clusters in the bombarded tip shown in Fig. 11(b). The tip

Fig. 11a

Fig. 11b

was not bombarded in the close packed direction but four clusters are clearly seen in this direction on either side of the tip. It may be that more energy transfer took place in this direction.

11. Mobility of interstitials at low temperature.

Little work has been done on the annealing of defects in tungsten at low temperatures. Kinchin and Thompson[5] have investigated the annealing behavior of neutron irradiated tungsten at low temperature by electrical resistivity measurements. In general, the annealing process in irradiated substances is complicated and not yet well understood. In the present work an attempt has been made to study the mobility of interstitials or their clusters at low temperatures. Experiments have shown that in tungsten the interstitials can migrate even at about $21^{\circ}K$, and a rapid mobility occurs in the region $90^{\circ}K$ to $100^{\circ}K$.

The interstitial migration at $21^{\circ}K$ is observed when a tip is bombarded at this temperature and then the beam turned off and the image observed. It is very often observed that some interstitials come out on the surface of the tip. That these new atoms are interstitials produced by bombardment is confirmed by the fact already mentioned that in a helium ion image not a single change occurs for a long time if it is allowed to stand without bombarding the tip.

Interstitial migration at somewhat higher temperatures has been studied in two ways. The main difficulty in such experiments is to determine the temperature of the tip. In the absence of any suitable present method to find this temperature, first experiments were done by applying small voltages across the tip leads, a

process done by the same power supply used for applying high voltage. After bombarding the tip it is photographed, then .1 to 1.5 volts are applied across the tip heater loop. Such experiments show that as the voltage is gradually increased, many new interstitials come out on the surface while some of the previous ones remain and some evaporate. If in one case the tip was heated to about 80^0K, the feature to be noticed was that on the entrance side the new interstitials and those removed are almost equal in number, while on the exit side most of them are new interstitials. It appears that many knock-on atoms were a few atomic layers deep on the exit side and came out on heating, while the interstitials on this side appear more tightly bound. Maybe they were one atomic layer inside as already explained in Sec. 6. On the entrance side, it appears that many interstitials were on the surface and were quickly removed. In such experiments, when the tip is gradually heated to a higher temperature all interstitials on the surface move away and finally even the field evaporation of the different crystal planes occurs.

In order to see if a temperature exists at which the inter-stitials migrate more rapidly, the following experiment was done. As usual the tip was bombarded with liquid hydrogen in the cold finger. The time was noted when liquid hydrogen was filled in the cold finger. Then the hydrogen was allowed to evaporate. When almost all of it evaporated the interstitials coming out on the surface were observed and each one was registered on a Varian graphic recorder by a push button switch. The quality of the ion image gradually deteriorates as the temperature increases until it becomes completely blurred. The recording gave the number of

interstitials moving out as a function of time. Thus, it is known that the most rapid migration of the interstitials takes place a certain time after the liquid hydrogen was filled in the cold finger. Next, liquid hydrogen is filled up to the same level in the cold finger, with the same He pressure in the microscope tube to have the same radiation losses. The liquid hydrogen is again allowed to evaporate and the time is noted. When all of it has evaporated and the temperature of the cold finger has risen, a pentane thermometer reading down to $-200^{\circ}C$ is used for observing the further increase of temperature with time. About a dozen interstitials appeared during the heating. It should be mentioned that all events occurring on all parts of the screen cannot be simultaneously seen visually and so the number recorded must be lower than the actual number. In this experiment the temperature range corresponding to most rapid migration of the interstitials to the surface was from $90^{\circ} - 100^{\circ}K$.

To check the above result, the quality of tip image at which most rapid migration of the interstitials takes place can be taken as an indicator of its temperature. In a later experiment the ion image is obtained with liquid nitrogen in the cold finger and as the nitrogen evaporates away, the temperature at the bottom of the cold finger is indicated by the pentane thermometer. That temperature is noted at which the image quality is the same as when rapid migration of the interstitials was observed by evaporating liquid hydrogen and increasing the temperature of the tip. This experiment indicated that the rapid migration of interstitials to the surface occurs around $95^{\circ}K$. Thus it is concluded that the

first rapid migration above liquid hydrogen temperature is actually between $90^{\circ} - 100^{\circ}K$. It is planned to make later more accurate temperature determinations by measuring the resistivity of the central part of the heater loop.

The experiments in which the tip temperature is increased by applying a small voltage across it, have shown that the number of interstitials coming out depends on its previous bombardment. If the tip is bombarded for a long time or if it is bombarded with the heavier atoms of Hg, very small number of interstitials come out on heating. The explanation seems to be that with more damage inside, the interstitials are trapped there and are unable to migrate far enough to the surface.

12. Bombardment with no high voltage at the tip.

In all experiments described so far, the tip was kept at high voltage during its bombardment. The main reason is that when the tip is kept at the high voltage necessary to get the helium ion image, no contamination gases can reach it. Thus the surface remains clean throughout the experiment. When the tip is hit by the helium atoms, the changes taking place on it can be observed simultaneously. The disadvantage, as already mentioned before, is that the tip surface is at high outward stress due to the electric field. Working with high voltage on becomes necessary because of greased ground joints and the consequent contamination gases.

Some experiments were done to see the difference when the tip is bombarded with no high voltage at it. First to check the vacuum condition and the changes obtained on the surface of the

tip, the high volt was turned off for a particular time and the
helium ion image was obtained again. Then the voltage was turned
off for the same time again, the tip was bombarded and the image
obtained. In such experiments the damage produced was more as all
helium ions, in addition to neutral atoms, also hit the tip. Fur-
ther, the important observation was that as the voltage is increased
to the value for getting a helium ion image, a large number of
bright points are seen to come out from the inside during the first
one or two seconds and they then stay on the surface. Otherwise,
whenever the voltage is increased to obtain the image such bright
points appear on the surface, but being due to contamination gases,
they are torn off as the voltage reaches the value of good He ion
image. Then only a clear He ion image of tungsten remains on the
screen. But in this case these bright points on the screen come
out suddenly at the He ion image voltage and then stay. Thus it
is thought that these are the displaced tungsten atoms lying
few atomic layers deep and are pulled out on the surface as a result
of the field. Some stay there while others leave. The same
phenomenon must occur when the tip is bombarded with the high
voltage at it. It is hard to estimate the actual number of inter-
stitials or vacancies even on the surface because of replacement
collisions. In such collisions the interaction between a moving
interstitial atom and a stationary atom results in the displacement
of the stationary atom and leaves the interstitial with insufficient
kinetic energy for it to escape from the vacancy. Then this atom
will remain in the vacancy, dissipating its kinetic energy through
lattice vibrations. The threshold energy of such collisions is small

and calculations in the case of Cu^{14} have shown that the number of replacement collisions exceed that of displacement collisions. Such collisions can result in observable effects in polyatomic alloys or compounds but not tungsten.

When the high voltage was turned off for five seconds and then the photograph taken four new and 15 missing atoms were the result, all caused by contamination from the residual gas. Then the same tip was bombarded for five seconds at three microns He pressure. The changes are many and at least 75 new and 75 missing atoms can be counted. This number is almost twice of that which is obtained when a tip of about the same radius and same He pressure is bombarded with the high voltage on.

III. SUMMARY AND CONCLUSIONS

Almost all work in radiation damage has been based on the study of changes in the bulk properties of solids as a result of irradiation. These changes have been explained as a result of the production of vacancies, interstitial atoms and thermal or displacement spikes.

With the invention of the field ion microscope, it became possible to observe directly the atomic defects in metals. In the present work, the bombardment of tungsten tips at $21^{\circ}K$ by 20 kev helium atoms has been studied with a low temperature field ion microscope. The 20 kev He atoms were obtained by charge changing of helium ions accelerated from a Penning discharge.

The defects found are vacancies, interstitials and their clusters, and a disordering of atoms in a region of about

50 - 100 A diameter. This region may be the intersection of a thermal spike by the surface of the tip.

The number of neutral atoms hitting the tip per second ranged from one to 33. The number of displaced atoms appearing on the surface or one atomic layer deep have been counted and the total number of displaced atoms in the volume of the tip have been calculated from the hard sphere approximation. Surprisingly a large fraction of the calculated number of atoms displaced in the target volume appear on the surface. This is supposed to be the result of the high electric field of about 450 MV/cm at the surface of the tips, when it is bombarded and observed. Further, the surface itself acts as a sink for the defects which move by focussing collisions.

Tips of different radii (200A - 900A) have been bombarded, and the ratio of the damage on the entrance side of the beam and the exit side increases with increasing radius, indicating a range of the moving defects of the order of 500 to 1000 $\overset{\text{o}}{\text{A}}$.

The migration of interstitials or their clusters to the surface after termination of bombardment was studied by raising the temperature of the tip up to 110°K, and also at liquid hydrogen temperature. Some interstitials can move at 21°K and a rapid migration occurs in the region $90^{\circ} - 100^{\circ}$K.

The tips were also bombarded by much heavier atoms of mercury. The damage is very different. Vacancies and interstitials are produced but the number of regions in which disordering of atoms occurs are more than that with helium bombardment. Additionally, field evaporation of some atomic planes takes place. This is

explained as a result of field reduction of the energy barrier for the atoms to leave the surface.

All the above experiments were done with the high field at the tip in order to keep it clean. This produces a high outward stress of about 10^{10} dynes/cm^2 which causes some of the defects to disappear from the surface and to bring out others from inside. This is confirmed by bombarding experiments with the field off.

BIBLIOGRAPHY

1(a). F. Seitz and J. S. Koehler, "Displacement of Atoms
During Irradiation," in 'Solid State Physics',
Vol. 2, pp. 307-442, Academic Press, Inc., New York, 1956.

(b). G. J. Dienes and G. H. Vineyard, "Radiation Effects in
Solids," Interscience Publishers, Inc., New York, 1957.

2. E. A. Pearlstein, H. Inghan and R. Smoluchowski, Bull. Am.
Phys. Soc. 30, No. 2, 7 (1955) "cited by Seitz and Koehlar
in reference 1(a)."

3. G. Kinchin and M. W. Thompson, J. Nucl. Energy 6, 275 (1958).

4. M. W. Thompson, The Philosophical Magazine 5, 278 (1960).

5. E. W. Müller, Z. Physik 136, 131 (1951).

6. E. W. Müller, "Field Ionization and Field Ion Microscopy" in
'Advances in Electronics and Electron Physics' Vol. XIII,
pp. 83-179, Academic Press, Inc., New York, 1960.

7. S. K. Allison, Rev. Mod. Phys. 30, 1137 (1958).

8. E. W. Müller and K. Bahadur, Phys. Rev. 102, 624 (1956).

9. W. T. Leland and Roy Olson, Los Almos Scientific Lab. Report
LA-2344, Dec. (1959).

10. E. W. Müller, J. Appl. Phys. 28, 1 (1957).

11. N. Bohr, "The Penetration of Atomic Particles Through Matter,"
Kgl. Danske Videnskab. Selskab, Mat-fys. Medd. 18, 8 (1948).

12. G. H. Kinchin and R. S. Pease, "The Displacement of Atoms in
Solids by Radiation," Rept. Prog. in Physics 18, 1 (1955).

13. R. M. Walker, "Survey of Rad. Damage Thresholds,"
G. E. Lab. Scientific Report No. 1, AF CRC-TN-59-552.

14. J. B. Gibson, A. N. Goland, M. Milgram, and G. H. Vineyard,
Phys. Rev. 120, 1229 (1960).

PART 2. CORROSION OF TUNGSTEN BY WATER AND NITROGEN IN A FIELD ION MICROSCOPE

by J. F. Mulson and E. W. Müller

I. INTRODUCTION

Origin of the Study

Since its discovery in 1951[1] the field ion microscope has become an increasingly more useful tool in the study of refractory metals and their crystal structures. In 1957[2,3] the microscope was modified by incorporating a new specimen assembly which was attached to the body of the microscope by means of a ground joint thereby making possible rapid specimen changes.

When the specimen was cooled with liquid hydrogen, the contaminating gases were trapped on the cold surfaces, giving good vacuums even though the system was not baked. But a new phenomenon was observed when this new field ion microscope was operated at $77^{\circ}K$ with liquid nitrogen cooling. The periphery of a tungsten image was seen to be desorbing in an electric field of approximately 450 MV/cm. This was unusual since tungsten surfaces had been observed for several years at this temperature in baked-out field ion microscopes and were found to be stable.

This effect was found to be more pronounced in an experiment where photographic plates were introduced into the field ion microscope so that they would be exposed by the ion beam directly. In fact, direct photography turned out to be impossible even if liquid hydrogen was used for cooling the tip. Since photographic plates

are known to be hygroscopic, water was immediately suspected. A preliminary experiment showed that water could indeed cause this corrosion which shall be referred to as an etch.

The etch is seen to take place at a temperature of 77°K in a region where the electric field is 450 MV/cm. It is not immediately obvious how the water supply to this region is maintained since incoming molecules from space would be ionized far from the surface and travel to the negative electrode. One would also expect the molecules which could have approached the shank of the tip in the low field region to be bound too firmly for surface migration to take place at this temperature. A systematic investigation was begun to determine what the process or processes were which permitted this etch to take place.

Examination of the Problem

A preliminary experiment, where frozen water located in a side arm was warmed and released into a field ion microscope, showed that water would attack a tungsten surface. Since the etch is visible, the etching agent (H_2O, H, O, or OH^-) must reach that region of the surface which is being imaged by the helium ions. This means that the etching agent must exist as a neutral or negative particle in a region that has an electric field of such magnitude that helium atoms, whose ionization potential is 24.46 electron volts, are immediately ionized.

A neutral water molecule is attracted toward the specimen by the interaction of its dipole moment with the inhomogeneous electric field, but because of its low ionization potential (12.56 electron volts) the water molecule will become ionized far from the surface

and travel to the negative electrode. If one considers a hydroxyl ion (OH^-) which could possibly result from the dissociation of a water molecule in the high field, the ion would immediately become a neutral particle because of the low binding energy of the excess electron. The resulting neutral particle would then become positively ionized before reaching the surface, making it impossible for the etching agent to reach the surface from space.

The theory of field ion emission[3] shows that a particle whose ionization potential is greater than the work function of the metal being investigated cannot be ionized in a region close to the surface. The extent of this region depends on the magnitude of the field, the work function of the metal, and the ionization potential of the particle in the following manner:[3]

$$e F x_c \geq V_I - \varphi - \frac{e^2}{4x} + \frac{1}{2} F^2(\alpha_A - \alpha_I)$$

where x_c is the height of the forbidden region of ionization above the surface, F is the electric field, V_I is the ionization potential of the particle, φ is the work function of the metal, α_A is the polarizability of the particle before ionization, and α_I is the polarizability of the ion after ionization. This forbidden region of ionization exists because as the particle approaches the positive surface, the electrons in the particle lose potential energy and thus the kinetic energy they would have if they left the particle and traveled to the metal becomes less and less as the particle approaches the surface. If this kinetic energy were less than the Fermi energy of the metal, there would not be any unfilled states in the metal for the electron to occupy. Since by the Pauli exclusion principle two

electrons cannot occupy the same state, ionization cannot occur un-
less there is an unoccupied state of the proper energy within the
metal.

Thus, it is possible for a particle to move without being
ionized in these high fields if its motion is close enough to the
surface. This then allows a supply of particles to the image area
from outside of the perimeter. If there is to be any flow of
particles from the shank, there has to be a means of supplying
energy to them.

The following are the possible means for supplying the
necessary activation energy for the surface migration of the
molecules which are to be discussed in this investigation:

1. The activation energy for the surface migration of water
   on a tungsten surface might be so low that thermal
   migration is possible at $77^{\circ}K$.

2. The interaction between the dipole moment and the
   inhomogeneous electric field may be strong enough
   to reduce the necessary activation energy.

3. Energy can be supplied to the bound particles during
   collisions with the impinging molecules.

Scope

The initial investigation of this phenomenon was to deter-
mine whether or not it was a basically new effect since the
removal of surface atoms by impinging particles has been known
for some time in the form of cathode sputtering. When the effect
was found not to be sputtering, then it was necessary to find out

how the water molecules could reach that part of the surface where
the etch was seen to take place. The various processes suggested
in the examination of the problem were checked one by one. The
mechanism was suggested to be a chemical reaction where the
reaction products were too weakly bound to be stable in the high
electric field. This is a hypothesis that cannot be verified
until a mass spectrographic analysis of the desorbing particles is
made which was beyond the scope of this investigation. Such an
analysis is in the process of being carried out by R. Thomsen at
this laboratory.

II. APPARATUS

Considerations in Design

In a preliminary experiment water was frozen out in the side arm of a field ion microscope to provide a stream of water molecules to the tip. This type of water source was considered unsatisfactory since the source would have to be kept at low temperatures for long periods of time while the glassware was being baked at high temperatures. During this process the cold water source would have to be isolated from the system. This would then necessitate the use of an unbaked stopcock in the high vacuum region which would give rise to impurities in the water source and limit the vacuum which could be obtained with such a system. Therefore, it seemed adviseable to find another means of obtaining water vapor.

Crystals of gypsum ($Ca_2SO_4 \cdot 2H_2O$) are known to give off water when heated above 163° C. In order to test gypsum as a water source a side arm consisting of a steel ball valve, a cold trap, and a small tube containing gypsum crystals was attached to an existing field ion microscope shown in Figure 1. The microscope was first operated without the small tube which deflects the water molecules toward the screen. No etching occurred when the water was heated indicating that all the water was immediately frozen out on the liquid nitrogen cooled mantle. With the deflecting tube added the source worked very well and the ball valve was effective in starting and stopping
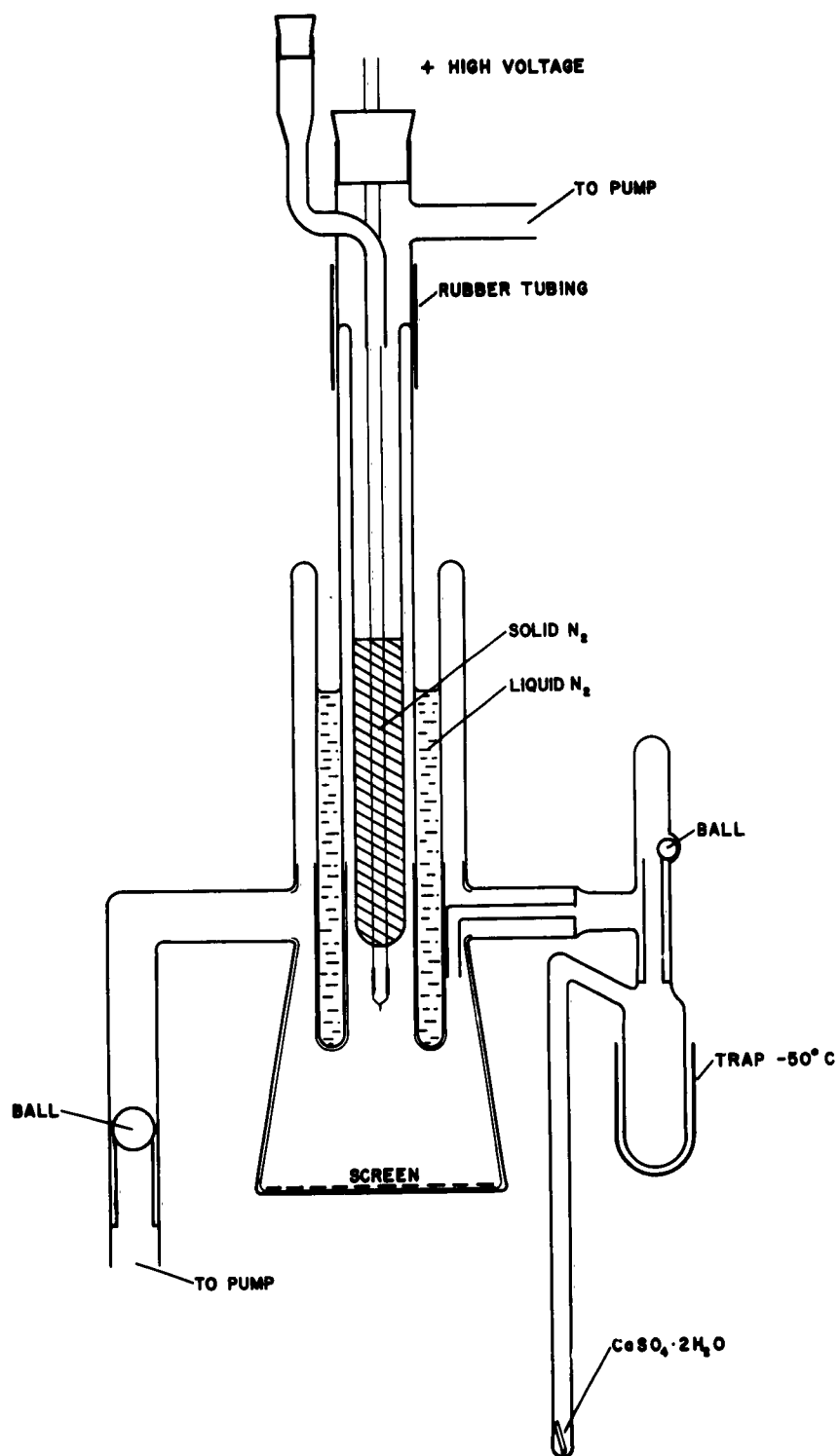
Figure 1.   Field Ion Microscope

With Water Source

the flow of water molecules. In Appendix B where the method of
constructing such a valve is described, there is a graph which
gives an indication of the leak-rate of these valves.

Some qualitative work was done with this microscope which
was inconclusive but did point out that a microscope was needed
which contained a water beam apparatus that could supply a
controllable and known amount of water to the tip.

A new field ion microscope, shown in Figure 2, was designed
which contained a water beam apparatus with the above mentioned
specifications. The gypsum crystals were stored in a small tube
out of the region to be baked but sufficiently close to be
radiantly heated by the oven, keeping condensables such as
mercury from gathering in this region during bake-out. At those
temperatures there was some outgassing of the crystals. A
further outgassing was done with a hand torch before cooling the
system. The small bulb at the end of the tube containing gypsum
was used to catch small particles that were sometimes carried off
with the water stream emitted by heating the gypsum. This was
necessary since the seat of the ball valve had to remain perfectly
clean. The temperature bath was used to establish and vary the
pressure in the beam chamber. A large copper block was used as
a heat sink and source to vary the temperature of the bath. The
steel ball valve was used to turn the water beam on and off. A
small well-defined orifice (1 $mm^2 \pm$ 1%) in the beam chamber was
used so that the number of particles leaving the beam chamber
could easily be calculated. A calculation of the beam flux at
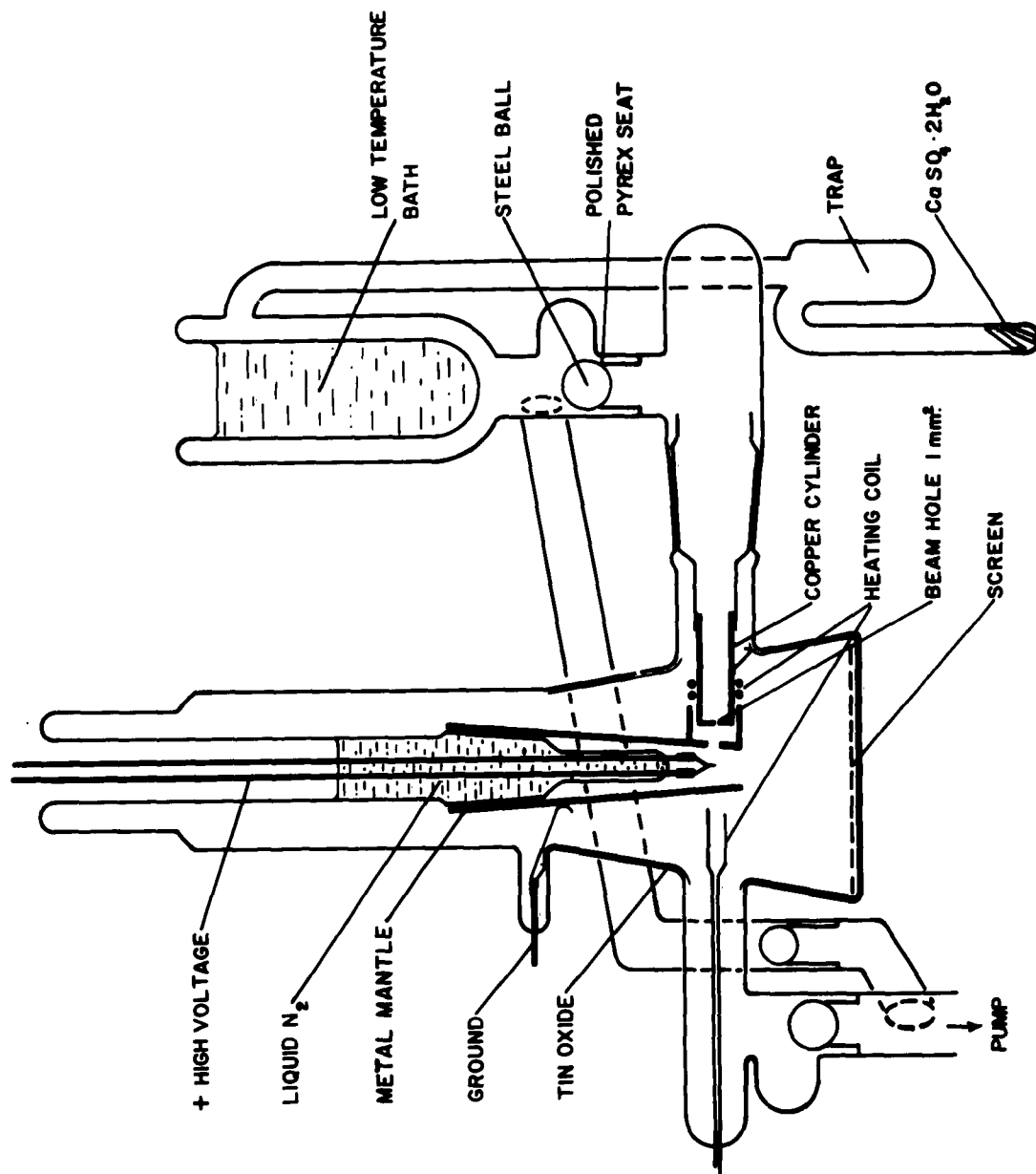
Figure 2.   Field Ion Microscope

With Water Beam

the tip is given in Appendix A. It was necessary to collimate the beam with a small hole in the cooling mantle in order to keep the beam from being scattered by warm surfaces. By confining the beam and surrounding the beam chamber with an extension from the cooling mantle, the possibility of scattered water molecules striking the tip was eliminated. But with the cold shell around the beam chamber, a heating coil had to be added to keep the temperature of the chamber above that of the temperature bath. This was necessary for two reasons. First, the known temperature of the bath had to be the pressure defining temperature so that the beam flux could be calculated; second, if there was water condensed in the beam chamber, the beam could not be turned off by closing the steel ball valve.

Gas Supply

Because of the need for high purity helium and also to eliminate the turning of stopcocks, helium was introduced by diffusion through vycor glass at about 650° C. See Appendix B for design and construction.

In order to retain the proper helium atmosphere for ion emission the bakeable steel ball valves were used.

Vacuum System

The remainder of the system was a high speed mercury diffusion pump with two liquid nitrogen traps in series and a mechanical fore-pump.

Three types of vacuum gauges were used, the Bayard-Alpert type ionization gauge, the McCleod gauge, and a field electron

microscope. The field electron microscope was used to check the
ionization gauge and also to help determine the residual contami-
nating gases. This microscope is sensitive to carbon, oxygen,
and nitrogen each of which gives a different and identifiable
emission pattern. The pressure was calculated from the time
necessary to deposit a monolayer of gas on the surface of the
emitter.

Photography

The ion microscope is capable of producing an image of a
metal surface in such detail that it is impossible for the
experimenter to assimilate more than a small fraction of the
information present during the experiment. Therefore, in
order to be able to reproduce the image accurately for further
study, photographic equipment and methods must be used that
preserve all the detail of the original image. A camera with
a F:1 lens corrected for 4:1 reduction was used with 103a-G
film. This is a high speed film sensitive in the green and
blue and was used to match the emission spectrum of the zinc
silicate phosphor on the screen.

Because of the low luminance of the image a compromise
had to be made between the grain and speed of the film. When
developed in ethol developer for six minutes, 103a-G was found
to have an ASA rating of about 3000. Even with this film
sensitivity and a F:1 lens, average exposure times of between
one and three minutes were necessary.

An exposure meter consisting of a 931A photomultiplier tube, 600 volt battery power supply, and an electrometer was needed to consistently insure negatives of the proper densities.

III.   EXPERIMENTAL PROCEDURE AND DISCUSSION OF RESULTS

Possible Etch Mechanisms to be Investigated Experimentally

There were two processes considered that could bring about the removal of tungsten atoms from their normally stable positions on the surface. One is a chemical process where the tungsten atom would combine chemically with the water molecule or its constituents and then the reaction products being too weakly bound to the surface would desorb. The other process is a physical one commonly known as sputtering. In this process the incoming particle transfers energy to the surface atom by means of an elastic collision. The energy of the incoming water molecule is supplied by the interaction of its dipole moment with the electric field surrounding the tip. A simple calculation (Appendix A) gives an energy of 0.97 electron volts. The maximum amount of this energy which can be transferred during an elastic collision is $\frac{4mM}{(M + m)^2}$ times the energy of the incident particle, where m is the mass of the incident particle, and M is the mass of the particle at rest. When m is a water molecule and M is a tungsten atom, 32.5% of the incident energy (0.32 electron volts) can be exchanged.

Investigation of the Constituents of Water

A small amount of pure oxygen was introduced into the vacuum system by heating a properly prepared silver ball to a temperature of about 600° C. The silver ball was prepared by cooling it from above 600° C. in the presence of oxygen. At high

temperatures the oxygen diffuses into the silver and is frozen in the lattice when the ball cools.

A field ion microscope containing oxygen at a pressure of 2 microns was operated with helium ions. No etch occurred.

A similar experiment was carried out with hydrogen and no etch occurred. The pure hydrogen was introduced into the vacuum system by diffusion through a palladium tube.

Experimental Determination of Delay Time

An experiment was carried out which measured the delay time between the turning on of the beam and the beginning of the etch. This was done by visual observation of the image. A stopwatch was used to measure the time between the opening of the ball valve and the observation of desorption of tungsten atoms from the periphery of the image.

Since the etch was thought to begin in the region outside of the imaged area, the tip was prepared for the experiment by first allowing the etch to move into that portion of the tip that was visible. Then the ball valve was closed stopping the beam, and the tip was heated to about 600° C. to remove the water. The surface of the tip remained unchanged since surface migration of tungsten does not take place at this temperature. The tip was prepared in the above manner so that the desorption of tungsten atoms would be visible when the etch began.

Measurements were made with tip temperatures of 77° K and 20.4° K. The time delay was found to be the same for both temperatures, i.e., the delay was independent of tip temperature.

Two different water pressures, $2 \cdot 10^{-3}$ mm. of Hg. and $2 \cdot 10^{-4}$ mm. of Hg., were used to measure the time delay. These two pressures were established by keeping the temperature bath at -68° C. and -82° C. A mixture of methyl alcohol and solid carbon dioxide was used to give a constant -82° C. The -68° C. was maintained by heating, or cooling methyl alcohol with a copper block of the proper temperature. This method gave a temperature variation of $\pm$ 2° C. The measured time delays were 2-3 seconds at $2 \cdot 10^{-3}$ mm. of Hg., and approximately 20 seconds at $2 \cdot 10^{-4}$ mm. of Hg. Other measurements are not reported because they were not reproducible with sufficient accuracy to render them valid. The bath temperature variations and the difficulty in establishing the start of the etch were responsible for the inaccuracies encountered. The most reliable measurement was made at -82° C. The start of the etch was considered to occur when the atoms desorbed at a constant rate. The first atoms desorbed randomly, hence delay times measured to the removal of these first atoms were not reproducible. Longer delay times increased the difficulty of determining a constant rate of etch because of the decreased etch rate.

The above measurements would not be valid unless the beam was known to start immediately after the opening of the ball valve. This was checked and verified by operating the microscope as a field electron microscope which can be accomplished merely by applying a negative voltage to the tip. Verification was possible since one can see in an field electron microscope small

amounts of materials deposited on the surface of a tip.

The delay before the beginning of the etch indicates that sputtering could not be responsible for the removal of the tungsten atoms. It also leads to the hypothesis that there must be a certain amount of water on the surface before the etch can start.

If one were to consider thermally activated surface migration, then it would appear that the first layer was bound too firmly to the surface and that second layer was migrating over the first layer. Such a hypothesis would need a delay time where the length of the delay would be the time needed for the completion of the first layer. The time required for the deposition of a monolayer would be inversely proportional to the water pressure and independent of tip temperature, which is consistent with experimental results.

Experimental Examination of Thermal Migration

An addition to the cooling mantle was made so that the possibility of thermally activated surface migration could be checked (Figure 3). The end of the tip was shielded from the water beam by a nickel plate with a hole in the center through which the tip protruded. The plate was electropolished to eliminate the possibility of field electron emission from the plate to the tip. The amount by which the tip extended through the hole eliminated the possibility of field activated surface migration, since the large field gradient at the surface occurs very close to the end of the tip.

METAL MANTLE

TIP SHIELD

TIP

BEAM HOLE
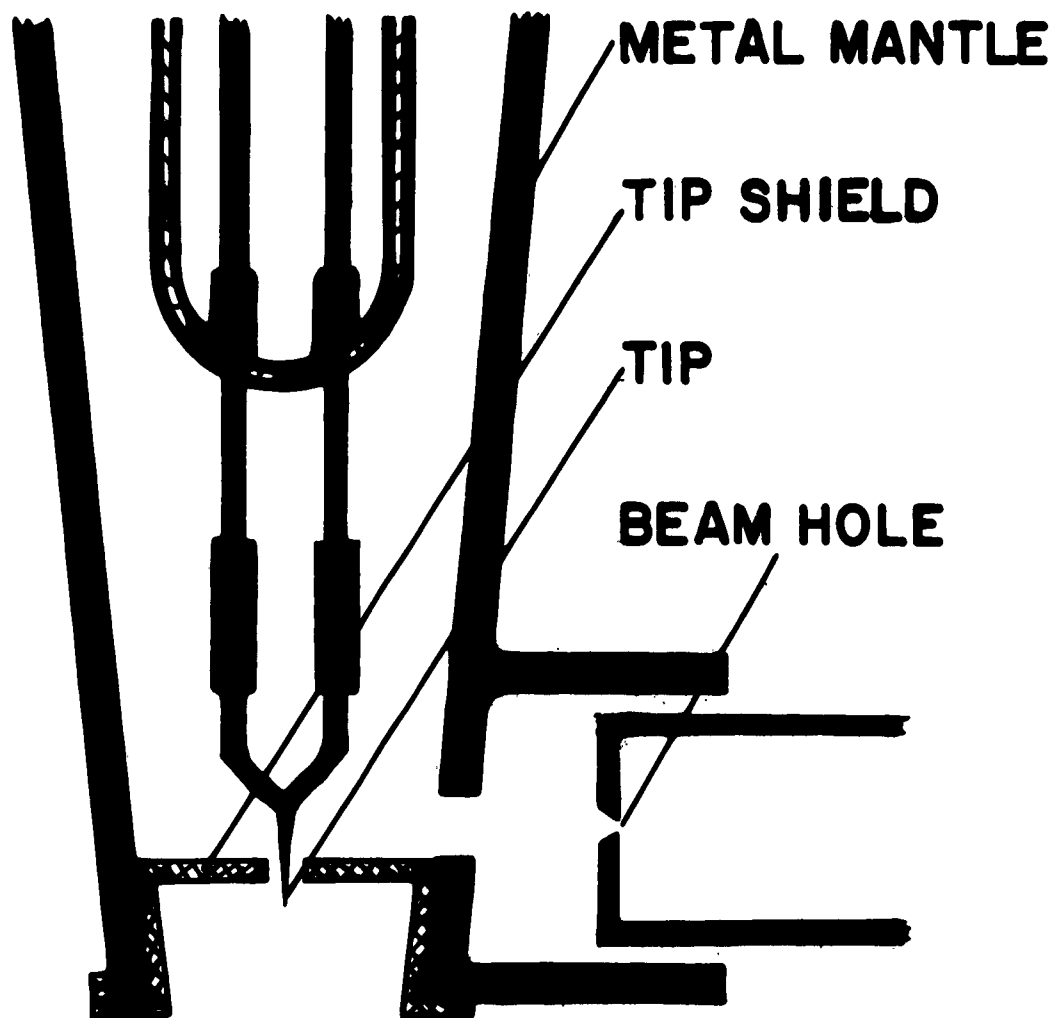
Figure 3. Cooling Mantle With

Tip Shield

The following results were obtained using the above described system. With the microscope cooled to 77° K the image was observed for ten minutes with the beam on. There was no evidence of etch. The tip was then heated to see whether surface migration would occur at slightly higher temperatures. No attempt was made to determine the temperature at which surface migration took place, since there are no accurate methods as yet for measuring the tip temperature in a field ion microscope. This experiment was set up to determine whether surface migration took place above or below 77° K. Since evaporation of tungsten would occur if the tip was heated with the electric field ion, the voltage was removed and heat was applied by passing current through the tip loop. The voltage of the loop circuit was recorded, but other unknown variables, such as contact resistances and thermal conduction, make it impossible to estimate the tip temperature from the recorded voltages. However, this data does suggest that the migration took place well above 77° K, as indicated by the following data:

Tip Voltage Volts	Loop Voltage Volts	Time Seconds	Results
7,600	0.0	--	Clean Image
0	0.0	5	
I 0	0.6	15	
0	0.0	45	
7,600	0.0	--	No Effect

	Tip Voltage Volts	Loop Voltage Volts	Time Seconds	Results
	7,600	0.0	--	Clean Image
	0	0.0	5	
II	0	0.72	15	
	0	0.0	45	
	7,600	0.0	--	Slight Coverage
	7,600	0.0	--	Clean Image
	0	0.0	5	
III	0	0.8	15	
	0	0.0	45	
	7,600	0.0	--	Heavy Coverage

The third column from the left is the length of time the tip and loop circuit voltages were applied. About one volt is sufficient to raise the tip temperature to 600° C.

It therefore can be concluded that thermally activated surface migration is not responsible for the supply of water molecules to the periphery of the image where the etch is seen to occur.

There are two other processes by which atoms or molecules could be made to move along the surface. One is field induced surface migration, the other is sputtering where the surface molecules are scattered along the surface by the impinging water molecules.

Experimental Investigation of Field-Induced Migration

If there were no field-induced surface migration, it would be possible to build up a layer of water on the side of the tip facing

the beam. The opposite side of the tip would be free of water since it is in the shadow of the beam. This effect is common in field electron microscopy where materials are evaporated onto the tip from a source off to one side.

The water beam was turned on for a short period while the tip was at zero voltage. With the beam off the voltage was raised to give the necessary field for the field ionization of helium. As the first spots of the image appeared there seemed to be more of an effect on the side facing the beam, but the surface rapidly equilibrated. This indicates that there is field induced surface migration, at least in that region which is visible.

The region of high electric fields is limited to the very end of the tip where the radii of curvature are small. An experiment was made which gives an indication of the smallness of this region.

The microscope was operated with the beam on for a short period. Ten seconds after the ball valve was closed, the etch stopped. The tip, while at zero voltage, was heated to redistribute the water from the shank. With the heat off the voltage was raised and etch was seen to occur for a very short period. The water was redistributed three more times with etch occurring. The fifth and sixth heating produced no etch.

This experiment shows that water was being supplied from outside of the image's perimeter. But because there is a delay time necessary for the beginning of etch, this region does not extend to the part of the tip which can be reached from space by the water

molecules, i.e., where the fields are less than the 200 MV/cm. which would ionize a water molecule.

As a hypothesis consistent with the experimental results it is proposed that the water molecules bound to the surface are scattered along the surface by collisions with the incoming water molecules. The rate of collisions then increases to a constant value, which occurs when the first layer on the surface is completed. This accounts for the difficulty in establishing the start of the etch.

IV. ADDITIONAL OBSERVATIONS

Tip Rupture Resultin^r from Water Etch

If water etch was permitted to continue, the image was ob-
served to grow smaller until an abrupt change took place in the
surface. The new image contained many structural disturbances
(Figure 4(c)). Figure 4(a,b) is an electron micrographic
comparison of the tip before and after water etch. After water
etch there is a noticeable constriction near the end of the tip.
If this constriction were to increase, it is conceiveable that
the large field-applied stress would have caused the tip to
rupture at that point. The new surface would then contain many
disturbances.

Nitrogen Etch

During the course of this investigation a field ion micro-
scope was operated with a helium-nitrogen atmosphere so that the
surface could be imaged at both 200 and 400 MV/cm. When the
electric field was raised to 450 MV/cm., nitrogen etch of a
tungsten surface was discovered. The nitrogen did not attack
the surface in a field of 200 MV/cm., in fact, good nitrogen
ion images of tungsten had been produced many times.

The nitrogen etch also took place at the periphery of the
image because of the low ionization potential of nitrogen.
Figure 5(a) is a photograph of a tungsten surface after water
etch, and Figure 5(b) is a tungsten image after nitrogen etch.
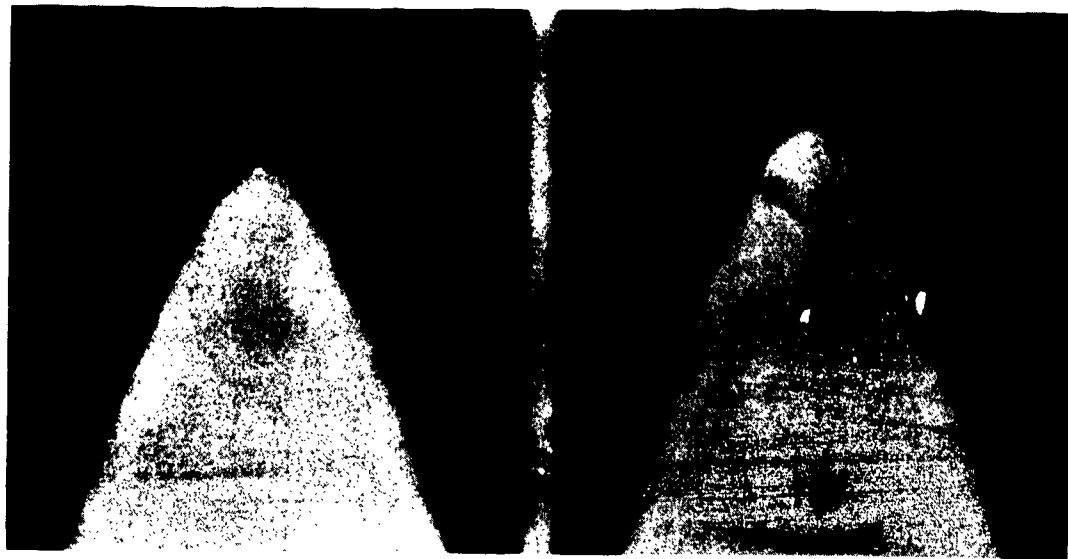
(a)

Tungsten Tip Before

Water Etch

(b)

Tungsten Tip After

Water Etch

(c)

Tungsten Image After

Tip Rupture

Figure 4.

(a)

Tungsten Image After

Water Etch

(b)

Tungsten Image After

Nitrogen Etch

(c)

Tungsten Image After

Nitrogen Etch

Figure 5.

In Figure 5(b) note the dark ring and abrupt change in symmetry where the etch stopped. The outer section of the image is characteristic of a tungsten surface after nitrogen etch. Figure 5(c) is a photograph of tungsten tip after nitrogen etch. The above surface was obtained by permitting the etch to progress at constant tip voltage. The image became smaller until it disappeared. Then the voltage was raised until the new image appeared. The photograph was taken before field evaporation. The new surface had a larger radius of curvature since a higher voltage was needed to produce the image. If the voltage is lowered as the etch progresses, it is possible to sharpen a tip.

Since etch changes the radius of curvature, the dark ring about the unetched region in Figure 5(b) could be the result of a discontinuity in the radius of curvature.

The study of etch resulting from nitrogen and other active gases[3] is being continued in this laboratory.

V. SUMMARY AND CONCLUSIONS

The pres-nce of small amounts of water at a pressure at the tip of about 10^{-6} mm. of Hg. causes corrosion of tungsten, platinum and probably other metals with the result that the surface atoms are removed in the high electric fields which are necessary for the operation of a field ion microscope.

It is proposed that the surface atoms are attacked chemically, with the reaction products desorbing in the high field. The water can be supplied to the etching site by migration from shank, moving close to the surface beneath the ionization zone. The force keeping them close to the surface is the interaction between the dipole moment and the inhomogeneous field. The activation energy is supplied to the bound molecules by collisions with the impinging water molecules. A mass spectrometer is being constructed in this laboratory in order to determine the chemical composition of the desorbing particles.

Nitrogen gas at a pressure of 10^{-6} mm. of Hg. will etch a tungsten surface in a field of 450 MV/cm. The etch occurs at the periphery of the image, and if permitted to progress at constant voltage, it will collapse the image until it disappears. With a nitrogen partial pressure of 2 microns the image will collapse entirely in about 3 seconds.

The nitrogen etch was similar to the etch observed in ground-joint microscopes. As a result of this investigation, getters were added to these microscopes making them operable at 77° K with helium ions.

BIBLIOGRAPHY

1. E. W. Müller. Z. Physik, 136:131 (1951).

2. E. W. Müller. Umschau, 57:579 (1957).

3. E. W. Müller. Advances in Electronics and Electron Phys., 13:83 (1960).

4. F. J. Norton. J. of App. Phys., 28, No. 1, 34 (1957).

PART III. MASS SPECTROSCOPY OF THE FIELD IONIZATION OF HYDROGEN NEAR A TUNGSTEN SURFACE

by T. C. Clements, E. W. Müller and B. J. Waclawski

I. INTRODUCTION

Field ionization of hydrogen was visualized by Oppenheimer[1] by predicting a probability of quantum mechanical tunneling out of the electron. The experimental verification was obtained when Müller[2] operated a field emission tip with reversed polarity in hydrogen gas of low pressure. The interpretation of these first observations with the field ion microscope was that at fields below 300 Mv/cm the emitter surface is directly involved in the ionization act, suggesting the occurrence of atomic hydrogen ions, and that beyond this field molecules would be ionized upon approaching the tip from the surrounding gas before actually reaching the tip surface. These ideas were substantiated with the mass spectroscopic observations by Inghram and Gomer,[3] who were able to measure the relative contributions of H^+ and H_2^+ over the entire field range. Their distribution curve further suggested the occurrence of fragmentation also of the approaching molecule either simultaneously or immediately after ionization, as evidenced by the predominance of H^+ in the high field region.

The present work originated from the need of a more detailed understanding of the field ionization process, as it turned out that Inghram and Gomer's field strength data were in error by a factor of two,[4] and that the image quality of field ion microscope pictures

was not quite as good as could be expected when compared to helium ion images. We also wanted to know if the ratio of H^+ to H_2^+ depended upon the pressure in a large ion yield dynamic gas supply system. The unexpected discovery of a fairly high concentration of H_3^+ ions which had not been reported by the previous researchers seemed also to justify a detailed investigation, which was extended to include field ionization of deuterium for further confirmation of of these observations.

II. EXPERIMENTAL

1. Apparatus

For the first part of this project, a $180°$, first order focusing, mass spectrometer was especially built. It consisted of a tube shown in Fig. 1, and later changed slightly to have a Faraday cage diagrammed in Fig. 2, a large electromagnet, dynamic gas supply, and a mercury diffusion pump system to maintain low pressure in the deflection chamber. The instrumentation is shown in Fig. 3 and was designed to display on a cathode ray tube screen a plot of the magnetic induction versus ion current, collected by the Faraday cage. The dynamic gas supply system[5] gives about 2 orders of magnitude increased ion currents compared to the conventional field ion emitter configuration.

In order to reduce field induced chemical reactions, particularly "water etch", a hydrogen purification system as shown in Fig. 4 was employed, relying mainly on diffusion through a palladium tube. Hydrogen was obtained as commercial dry tank gas, while deuterium was developed in an auxiliary glass vessel by the decomposition of

Fig. 1

Dashed Line shows Pole Shoe Outline

Conductive Coating

To Pump

Image Screen

Screen

Exit Slit

Ion Gun

Faraday Cage

Fig. 2

77
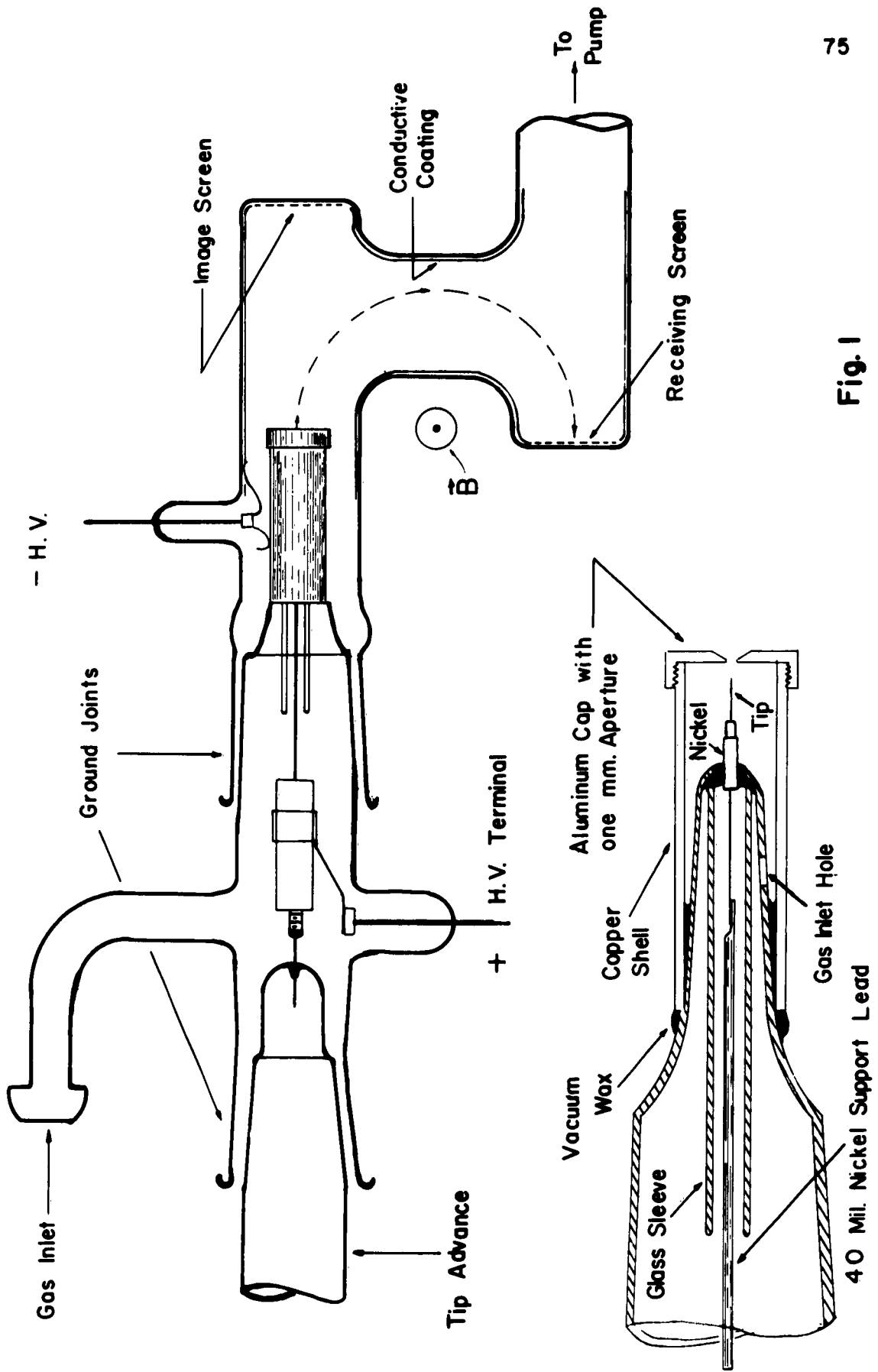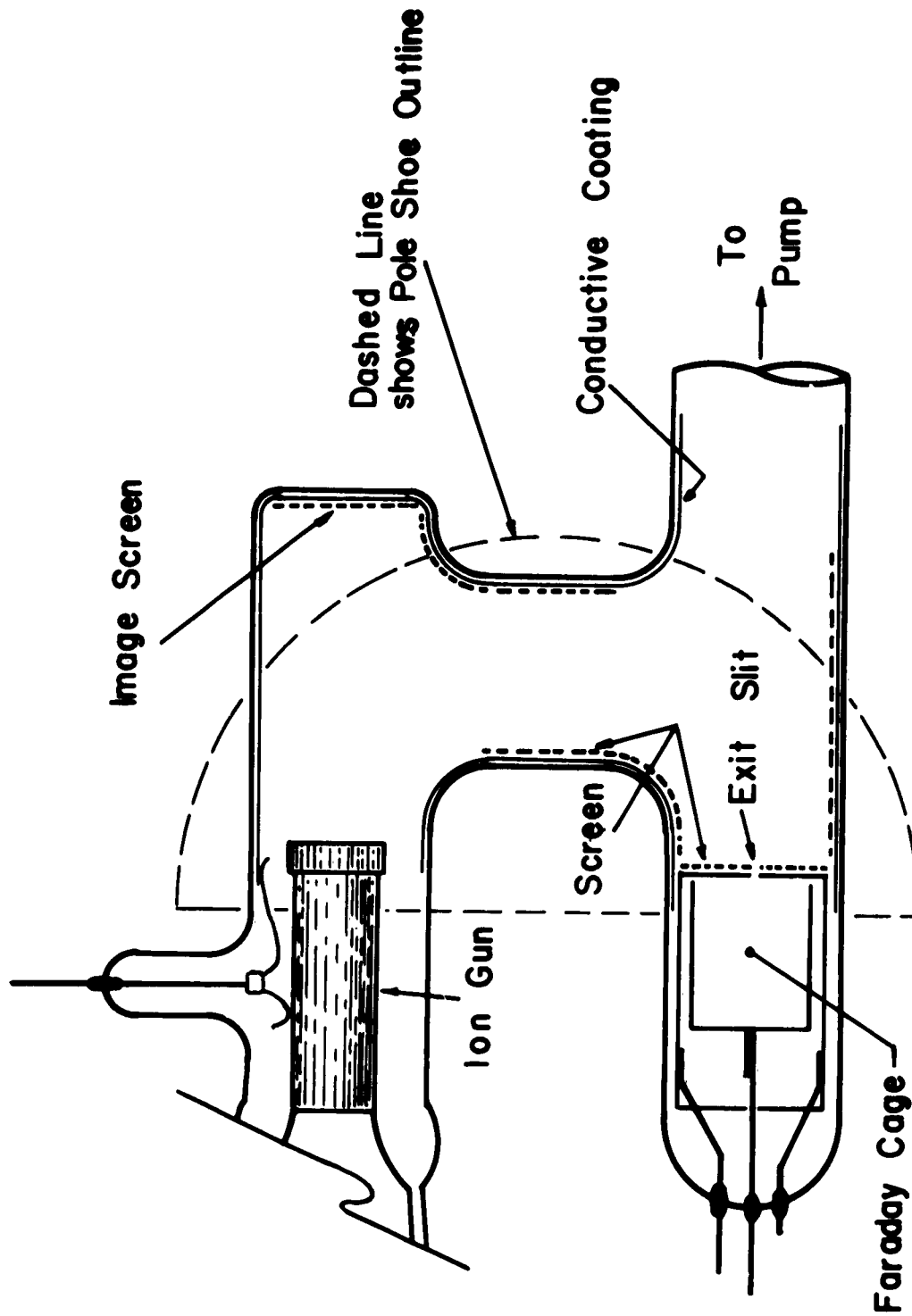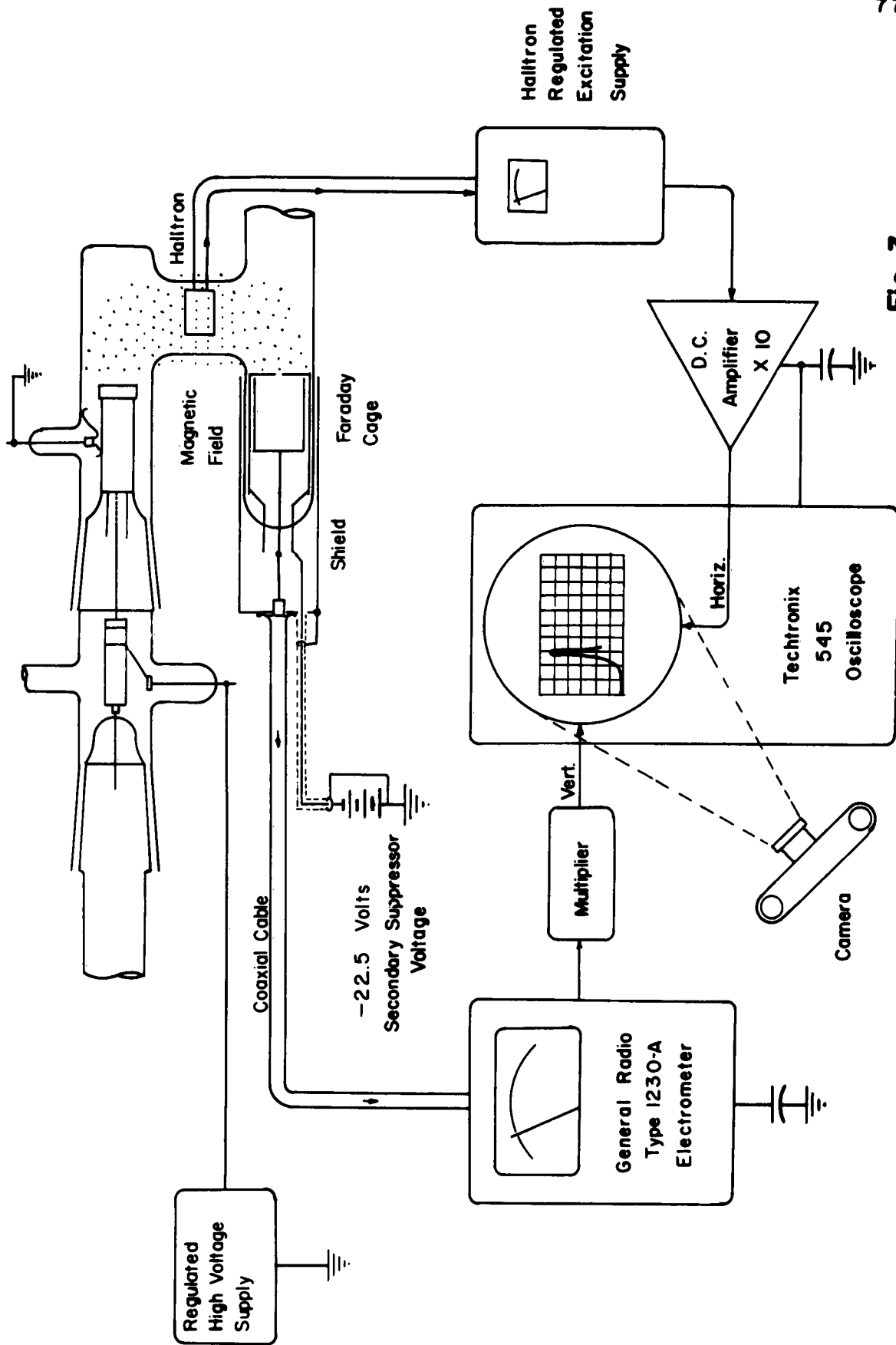
Fig. 3
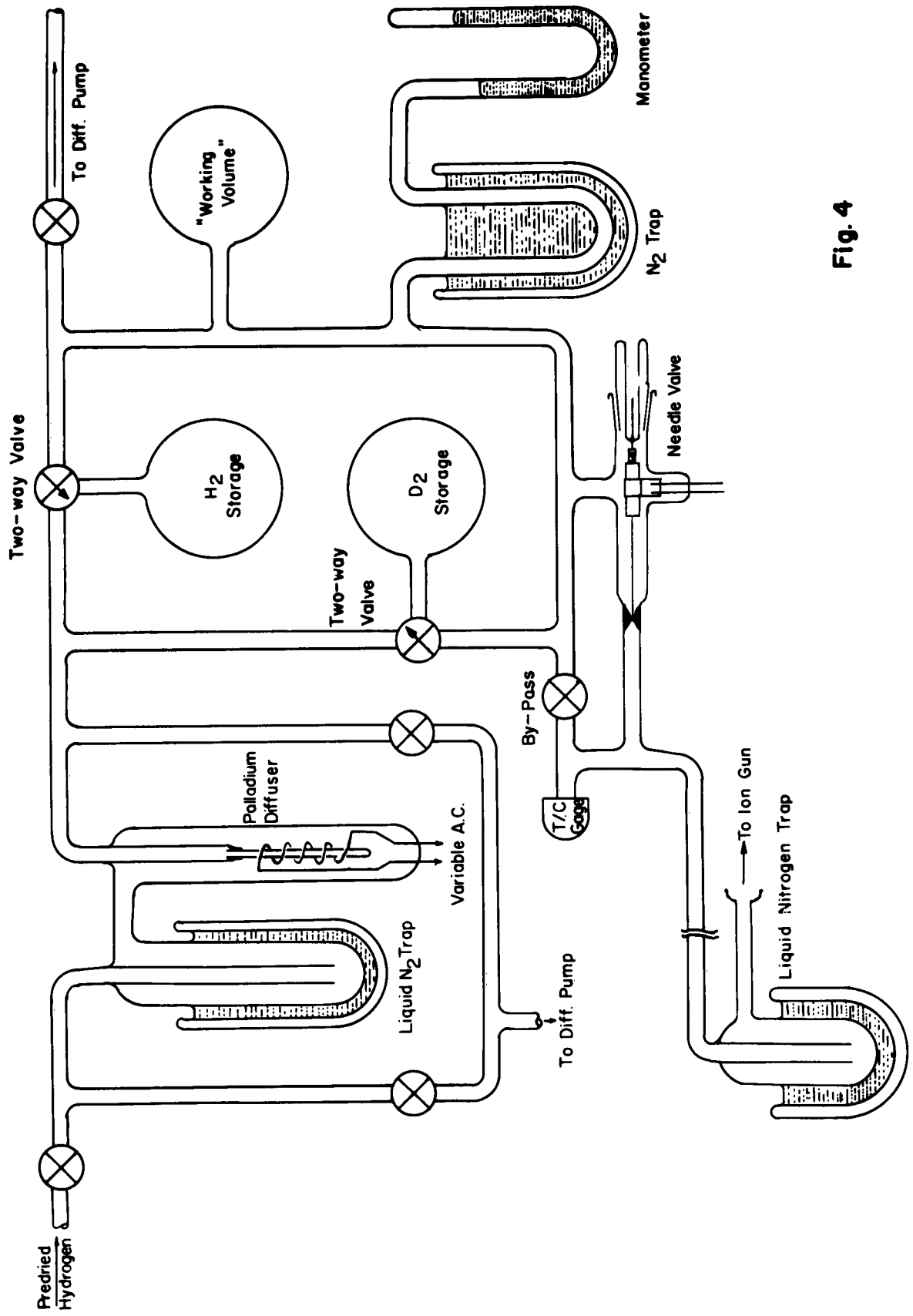
Fig. 4

heavy water with sodium metal. The presence of Apiezon-greased joints was not considered to have a significant effect on the measurements, as there was some field induced chemical etching of the emitter going on at all times, s that the surface was continuously renewed.

In the first experiments the tip was imaged by the magnetic field in the form of a slightly curved line, the brightness of which was measured with a photomultiplier. Since the efficiency of the phosphorscent screen is mass dependent, the relative abundance of the various masses could not be determined quantitatively. The Faraday cage used in the second set of experiments had a slit of one millimeter width which was slightly crescent shaped to fit the empirically determined beam shape.

Early in the course of this investigation it became evident that field induced tip etching presented a problem, so that the rapid changes in tip radius required fast recording of the mass spectrum. The sweep time used was usually 10 sec, so that the R-C time constant of the electrometer input circuit was small enough for proper recording of the mass peaks. Noise and other instabilities were several orders of magnitude below normal ion current measurements.

All the measurements with this 180^{0} mass spectrometer were made with the tip at room temperature. In order to keep the system simple no provisions were made for treating the retractable tip in the mass spectrometer itself. However, before inserting the ion gun head into the spectrometer tube, an auxiliary high vacuum system was used in which the emitter tip could be annealed through contact with a white hot tungsten wire.

2. Experimental Techniques

After a tungsten tip had been placed in the spectrometer tube, the system was pumped down to a pressure between 4×10^{-6} and 4×10^{-7} Torr, which took several hours. The electronic equipment was properly warmed up to ascertain stability. With the help of a thermocouple gauge and the needle valve hydrogen was then monitored to a pressure of 50 microns in the gas supply chamber. Spectra were taken at various tip voltages, and by turning off the magnetic field one could view the central part of the tip image on the image screen opposite the tip, in order to roughly have a relationship between applied voltage and field. It is known from field ion microscope work that the image turns blurred when above approximately 300 Mv/cm the ionization zone moves away from the surface. For the hydrogen field ion microscope the subjectively adjusted "best image field" is approximately 280 Mv/cm.

That field induced chemical etch was taking place was evident from 1) Variation of total ion current with time at constant voltage, without magnetic field; 2) Changing of the ion image at constant voltage to indicate gradually reduced field strength; 3) Variation of the mass spectra within a few minutes, characterized by changing in relative abundance of the hydrogen ion species. Efforts to stop this etch were not wholly successful in this apparatus, although nitrogen trapping of the supply gas directly before entering the spectrometer tube reduced the etching rate considerably, and long pumping times were also beneficial for more stable experiments.

As the work described in Part II of this Report has shown, etching continues even at liquid nitrogen temperature. Provision of liquid hydrogen cooling seemed too difficult for this apparatus design.

After the occurrence of the H_3^+ molecule ion was established with the apparatus above, two different field ion microscopes were modified to serve as a mass spectrometer for the hydrogen ion species. The first one of these had a static gas filling and permitted observations up to 3 microns pressure, and the second one used a dynamic gas supply.[5] These two microscopes served mainly to confirm the occurrence of the H_2^+ molecule under the cleaner conditions of an ion microscope, to establish more accurately the range of occurrence with respect to field strength and image details, and to extend the observation from room temperature to liquid nitrogen and liquid hydrogen temperature and over a pressure range from 80 microns down to .2 microns. The modification of the ion microscope was obtained by placing a movable slit formed by an about .05 mm wide gap between two 1 mm diameter tungsten wires at a distance of about 20 mm before the emitter tip. On the 4" image screen the slit wires appeared as about 12 mm wide dark bars with a light line between them across the entire image. As the slit assembly could be moved externally, it was possible to scan the entire image area. An external electromagnet placed below the slit level could then be turned on to deflect the shadow of the slit assembly by about 10 mm, and the image details in the slit image were split into the two or three masses of the hydrogen ions. With this device the ions coming from one individual surface atom in a protruding position could be mass analyzed. As these experiments were mostly of an exploratory nature, the screen image was photographed

at various voltages and the relative intensity of the 3 masses was only estimated. A quantitative determination of the abundances would have required microphotometry of the line intensities and a calibration of screen light output as a function of ion energy and mass.

3. Experimental Results

The general features of the experiments by Inghram and Gomer were confirmed. At low fields H_2^+ is predominant, but with increasing voltage the abundance of the proton increases. At about best image voltage (BIV), which corresponds roughly to 280 Mv/cm, the relative intensity of the proton beam equals the one of the molecular ion. At high voltages, when ionization occurs in free space above the surface, the relative H^+ abundance increases further, so that at about 500 Mv/cm, where field evaporation of the tungsten emitter sets in, the proton beam is about 7 to 10 times stronger than the molecular ion beam.

The occurrence of a mass 3 ion was unexpected, as it was not reported by Inghram and Gomer. Because of the rapid etch of the tip it was difficult to determine the exact field conditions for its appearance, but it could be clearly established that near best image voltage the abundance of H_3^+ was sometimes greater than of H^+.

Since the data obtained resembled those of Inghram and Gomer very closely (except for the appearance of H_3^+) it was concluded that the much higher pressure on our experiments did not change the ionization mechanism to any great extent. The ratio of abundance of H_1^+ and H_2^+ can serve as a measure of field strength, when the ion image of the emitter is not accessible. Inghram and Gomer's data

were re-plotted with the corrected field strength and by multiplying their peak height by the line width, as shown in Fig. 5. The general appearance of this pair of curves agrees with our observations, and the relative abundance of the H_3^+ ion has been added.

The appearance of the triatomic molecule ion was further confirmed by using deuterium and a hydrogen-deuterium mixture with about equal amounts of the isotopes. Within the limited accuracy due to uncertainty in field as a result of tip etching the ratio of H^+/H_2^+ equals that of D^+/D_2^+ in the entire accessible field range, and also D_3^+ appears near best image voltage. Typical mass spectra of the isotope mixture are shown in Fig. 7(a) for the case of approximately best image voltage, and in Fig. 7(b) for a much higher field.

The observations with the modified low pressure field ion microscope confirmed the previous observations under much cleaner conditions. Relative intensities of the species were estimated as functions of tip voltage, temperature and pressure. Only the tip voltage, or rather the field strength, seems to have any influence. Most measurements were made with the tip at 20^0K because of complete absence of field induced etching. At voltages below the subjectively estimated best image voltage (BIV), production of H_2^+ exceeded H_1^+. The latter increases with increasing voltage, until just below BIV abundances of H_1^+ and H_2^+ are equal. At this point traces of H_3^+ are noticeable with an intensity of less than 10% of the other ion spectras (?). Production of H_3^+ reaches a maximum of about 50% of H_2^+ just above BIV, and then disappears fast with further increased voltage. H_2^+ production increases only gradually, while the abundance

Fig. 5

Fig. 6a

Ions at high field (350 Mv/cm)

Fig. 6b

Ions at slightly above best image field (300 Mv/cm)

Fig. 6c

Ions below best image field (260 Mv/cm)

Fig. 7a

Deuterium-Hydrogen Mixture at low fields

Fig. 7b

Deuterium-Hydrogen Mixture at high fields
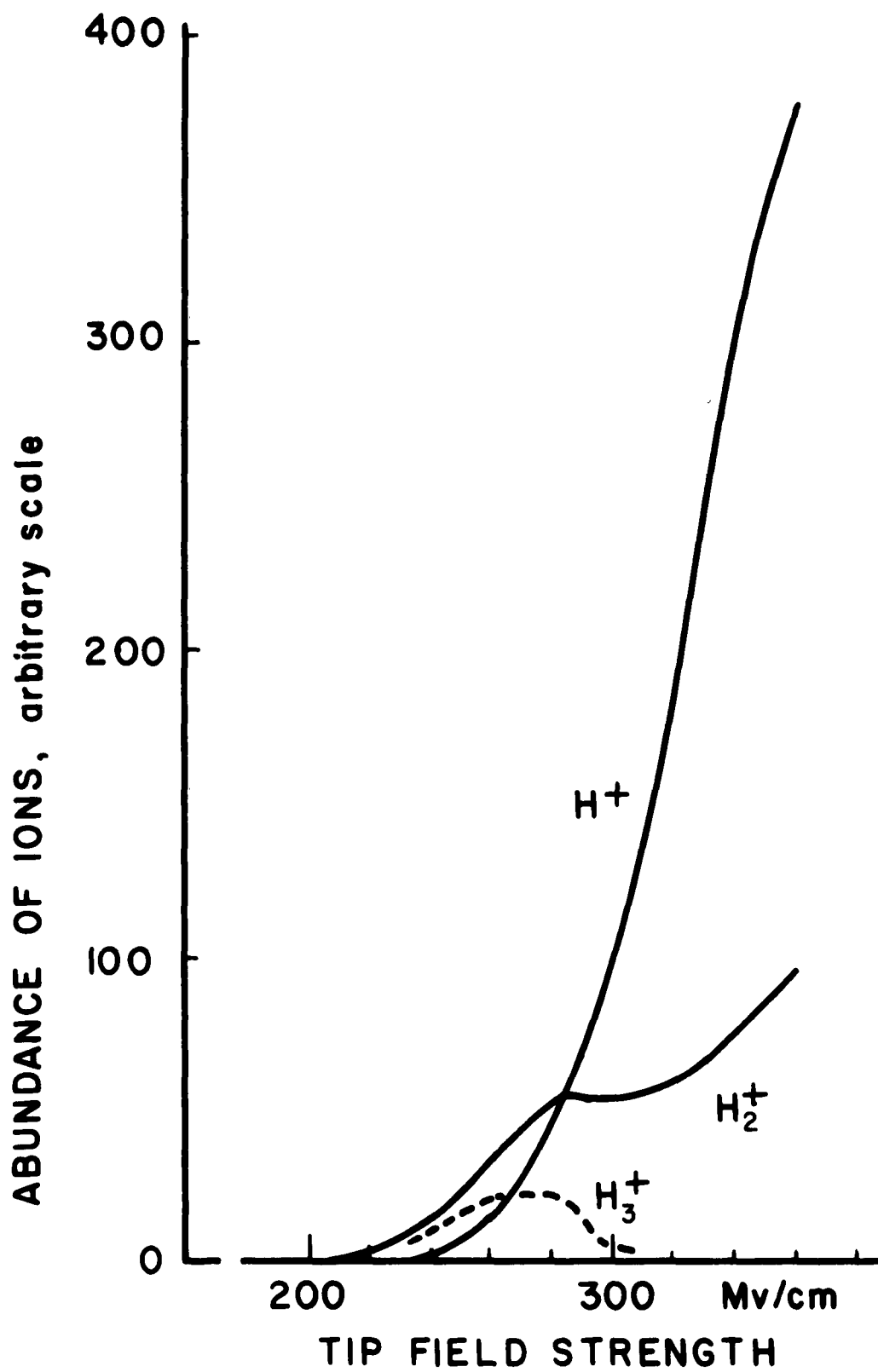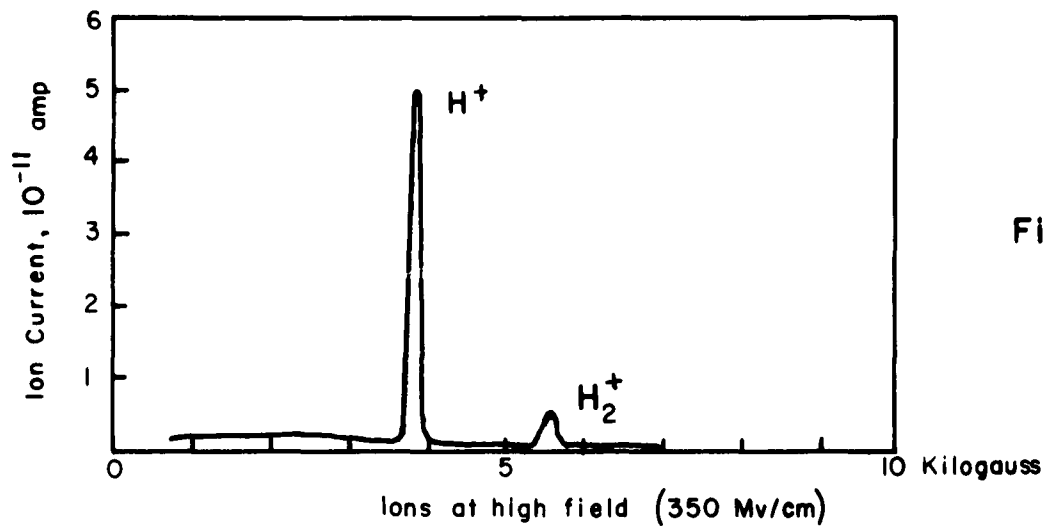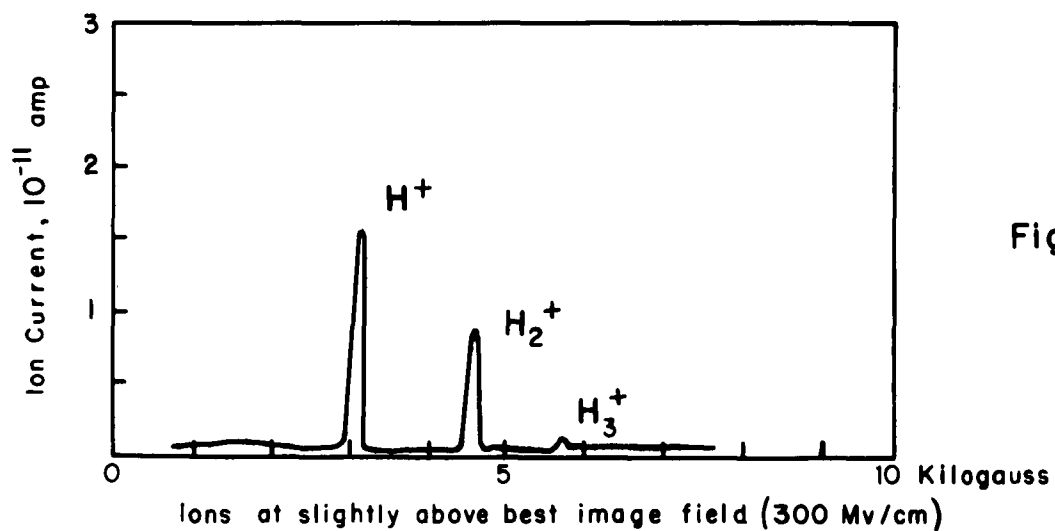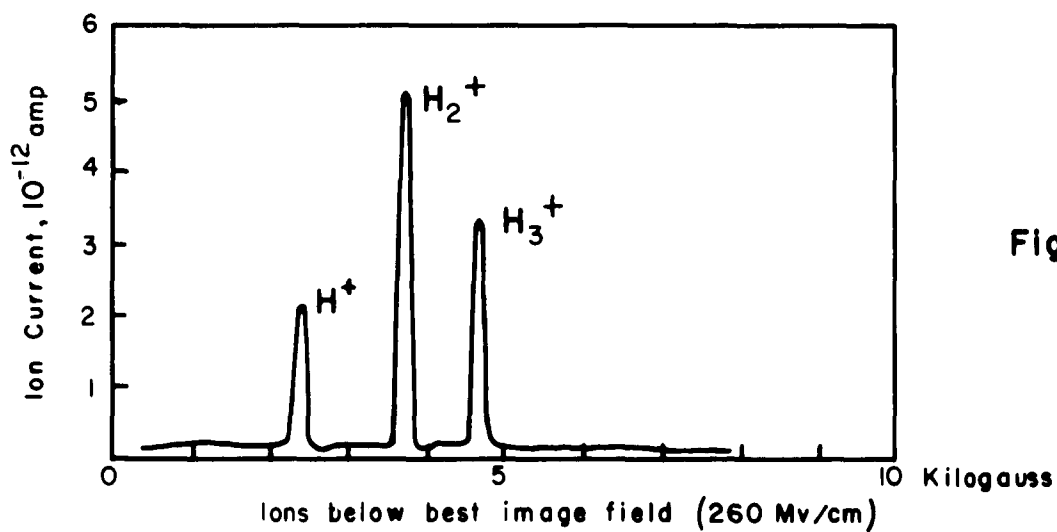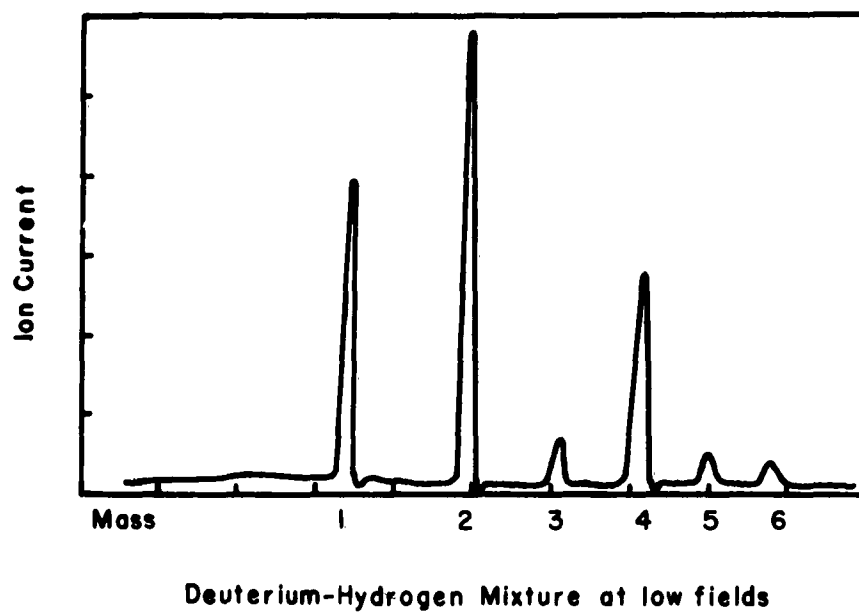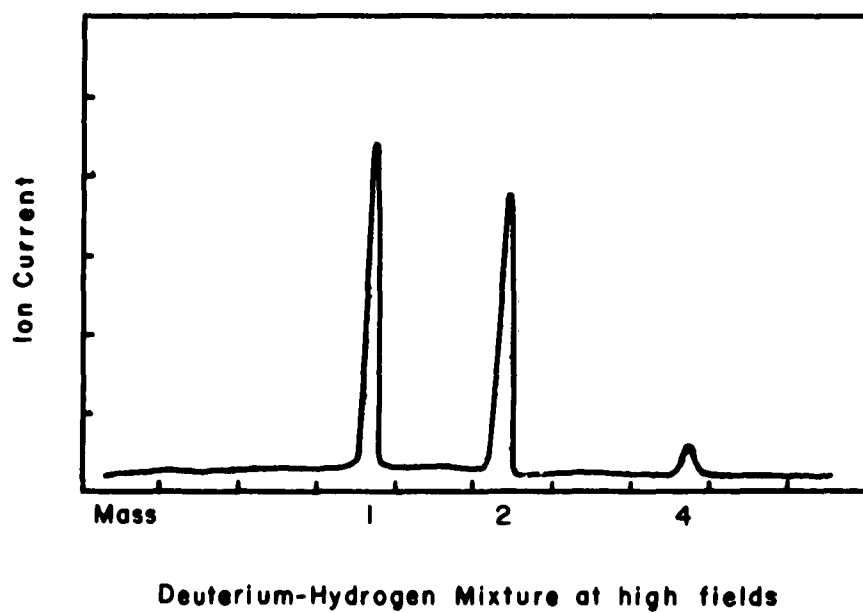
of H_1^+ goes up to read about 10 to 7 times the intensity of the H_2^+ ion at fields near 500 Mv/cm.

One particularly interesting observation was made with the ions coming off some single protruding tungsten atoms at a net plane edge. When the voltage was increased from the low field region, the intensity of H_1^+ dropped sharply, and the equivalent intensity of ions now appeared as H_3^+. Slightly above BIV the H_3^+ spot disappeared and H_1^+ began to rise sharply in intensity. This behavior is reproduced here in the photographs Figs. 8(a), (b) and the estimated intensities of the species originating above one single tungsten atom are shown in Fig. 9.

If the entire ion image is deflected by the magnet and the voltage is near BIV, the individual atom images are split into the masses 1, 2 and occasionally 3. The latter does not appear at all atoms in one photograph, which indicates that the local field strength was different at the various sites. The intensity ratio of the mass 1 and mass 2 image may serve to determine the effective local field above each depicted atom. The image also shows that there is no significant difference in apparent atom diameter in the two or three ion images of the same atom, indicating that the resolution under exactly identical conditions is not dependent upon ion mass.

There was practically no difference in the relative abundances of the three hydrogen ion species at the three temperatures used in these experiments, $21^{\circ}K$, $77^{\circ}K$, and $300^{\circ}K$. Also, the pressure varied between .5 micron and 80 microns did not change the relative abundances. However, at a pressure of .2 microns where the visual

Fig. 8a

Hydrogen, 12000 Volts, BIV.
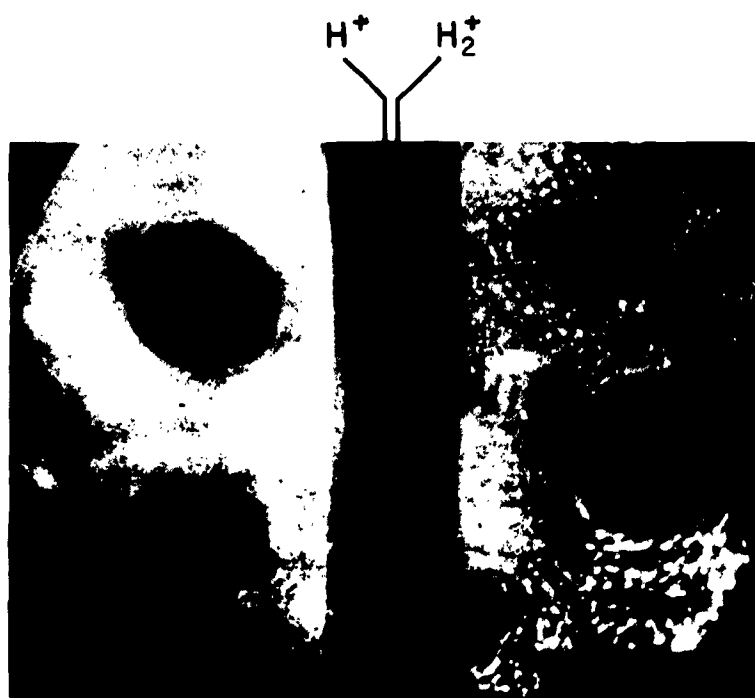
Fig. 8b

Hydrogen, 13000 Volts
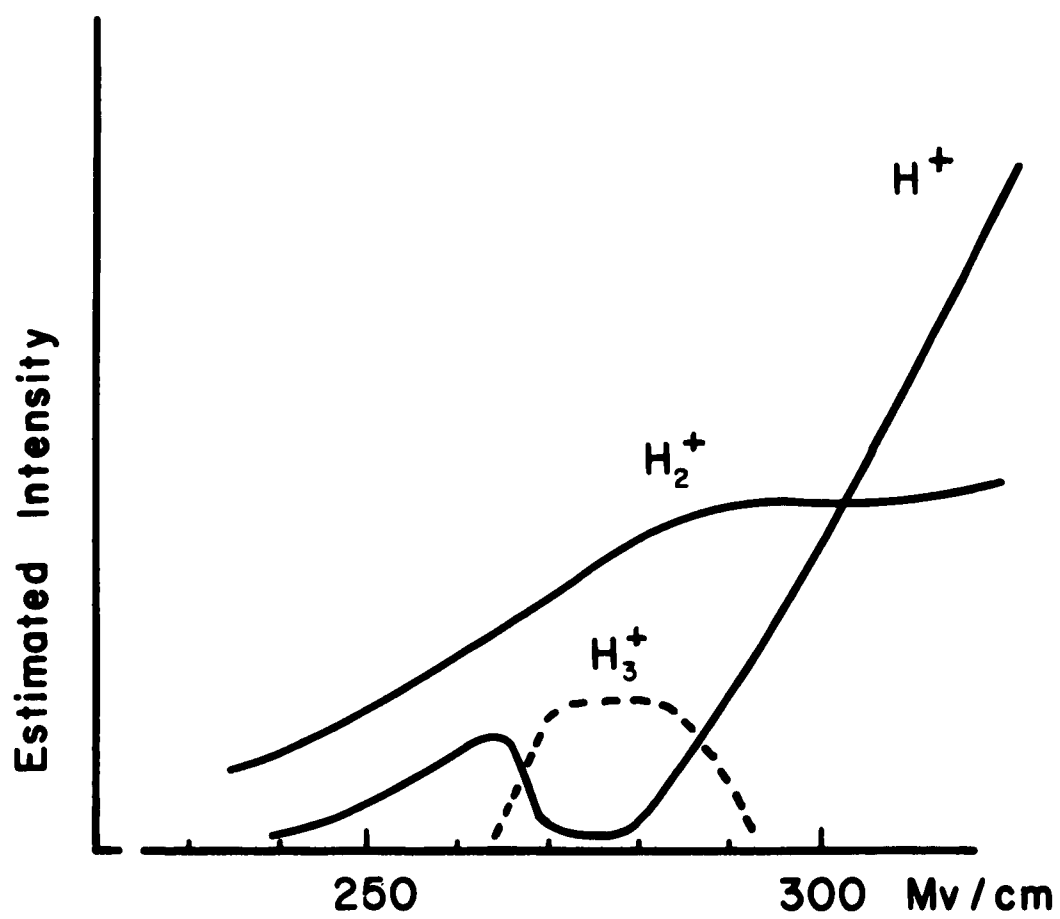
Fig. 9

observation was already difficult because of the low intensity, the intensity of H_3^+ reached a maximum of only 10% of the intensity of H_2^+. This points to the possibility that at still lower pressures H_3^+ may not be formed at all which could explain the failure of Inghram and Gomer to detect this species.

SUMMARY AND CONCLUSIONS

The experimental facts found in this investigation can be summarized as follows: H^+ and H_2^+ occur in the entire field range which is determined at the low side by the onset of noticeable ionization at about 200 Mv/cm, and at the high side by field evaporation of the tungsten emitter at above 500 Mv/cm. H_2^+ is predominant at low fields up to the best image field. When above this field the location of the ionization process moves away from the surface, the H^+ abundance exceeds H_2^+ more and more until it is about 7 to 10 times above H_2^+. The H_3^+ ion only appears in a narrow field range near best image field. Observation on a single atom indicates that H_3^+ is formed at the expense of H^+. The relative abundance of all three ion species is not noticeably dependent upon temperature in a range of $21^\circ K$ to $300^\circ K$, and also not upon pressure in the range from .5 to 80 microns. At lower pressures the H_3^+ ion is less abundant, and it may practically vanish below .1 micron.

The interpretation of these observations is difficult because of the possibility that several processes are involved, and because of the inhomogeneity of the local field distribution above the surface. Predominance of H_2^+ at low fields indicates that the H

atom which is present at the surface due to dissociative chemisorption participates only in a limited way in the field ionization act, despite the fact that its ionization potential is lower than that of H_2, and that because of its lower polarizability, its hopping height would be higher than that of H_2. It may be assumed that H atoms are more tightly bound, while H_2 molecules are diffusing abundantly over the surface on a hopping motion,[6] providing for the production of H_2^+ by field ionization. The reaction[7]

$$H_2^+ + H_2 \longrightarrow H_3^+ + H \qquad (1)$$

is unlikely to cause the formation of the triatomic molecule ion, as the resultant H should be easily ionized too, while the experiment shows that H_3^+ is produced at the cost of H^+. More likely is, then, the reaction

$$H_2 + H^+ \longrightarrow H_3^+ \qquad (2)$$

although this reaction is also known to lead to $H + H_2^+$. Above BIV conditions the latter process seems to be more probable, with the resulting H being ionized and the resulting H_2^+ dissociating to form $H^+ + H$, thus providing more H for subsequent ionization and increasing further the abundance of protons in the high field range. Most of the protons created at high fields come, however, from the dissociation of the H_2^+ molecule ion in the high field. The large abundance of the mass 5 molecule ion in the hydrogen-deuterium mixture suggests the mechanism

$$D_2 + H^+ \longrightarrow HD_2^+ \qquad (3)$$

and proves that with hydrogen alone the formation of H_3^+ proceeds according to Eq. (2).

It is planned to continue some of this work. Particularly the quantitative analysis of the abundances of the species in H_2-D_2 mixtures as observed under the better defined field - and cleanliness conditions of the modified field ion microscopes will give more insight into the mechanisms of field ionization and the influence of the metal surface.

BIBLIOGRAPHY

1. J. R. Oppenheimer, Phys. Rev. <u>31</u>, 67 (1928).

2. E. W. Müller, Zeit. f. Physik <u>136</u>, 131 (1951).

3. M. G. Inghram and R. Gomer, J. Chem. Phys. <u>22</u>, 1274 (1954).

4. E. W. Müller, "Field Ionization and Field Ion Microscopy", in Volume 13 of "Advances in Electronics and Electron Physics", Academic Press, 1960, pp. 83-179.

5. B. J. Waclawski and E. W. Müller, J. Appl. Phys. <u>32</u>, 1472 (1961).

6. E. W. Müller, J. Appl. Phys. <u>28</u>, 1 (1957).

7. D. P. Stevenson and D. O. Schissler, J. Chem. Phys. <u>29</u>, 282 (1958).

PART IV. AN IMPROVED METHOD FOR ELECTROPOLISHING FINE TIPS FOR FIELD ION MICROSCOPY[‡]

by Yuzo Yashiro and E. W. Müller

Etching and electropolishing of field emitter tips, particularly with radii well below 1000 A as desirable for field ion microscopy, is an empirical art. The most commonly used recrystallized tungsten wire has often an [011] oriented axis, and as a result of the twofold symmetry around this axis undesirable blade shaped tips are obtained when the attack of the etchant is too mild so that the various crystal planes are dissolved at different rates. In order to apply the high current densities which are desirable for non-discriminating electropolishing the use of current pulses as obtained by a condensor discharge was found to be practical. The circuit used is shown in Fig. 1. The best values for capacitance and etching voltage as well as electrolyte has to be chosen empirically for each tip material, and the optimum voltages may even depend upon the structure of the specific tip metal, e.g. its state of recrystallization, or cold working. In the equipment used the capacitance can be selected in 4 steps from 220 μF to 2200 μF, and the voltage is continuously adjustable between 0 and 70 volts. When a 4 mil tungsten wire is etched in concentrated KOH, using a capacity of 220 μF, the peak currents in the condensor discharge are 1 amp at 60 volts for rapid pre-etching, and 0.2 amp at 10 volts for finishing the tip, with a half time of the current pulse of 50 milliseconds.

[‡]This paper was presented at the Field Emission Symposium, Williamstown, Massachusetts, August 1961.
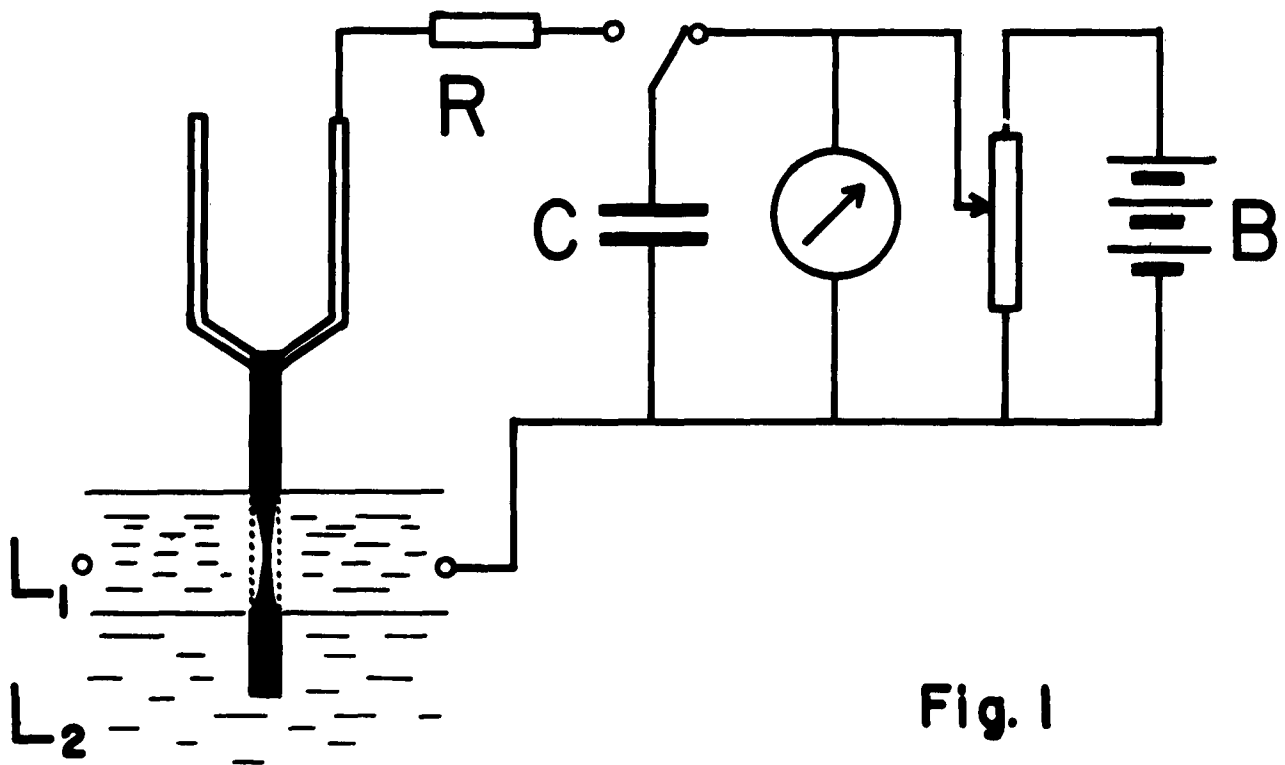
Fig. 1

When the tip wire is immersed for a length of some 5 mm a long taper with a very fine tip radius results. However, a too slender taper has the disadvantage of poor heat conduction from the supporting loop. It appears preferable to produce a concave shaped taper, which can be achieved by immersing the wire to a depth of only one milli- meter or less. The tip crystal structure is often heavily damaged at such a short distance from the end by the cutting process. It is therefore better to discard the cut end of the wire by etching the tip further away in an undamaged region. This is most con- veniently done by providing the etchant liquid in form of a thin layer L_1 floating as an insulating liquid of higher density L_2, as schematically shown in Fig. 1. It is convenient to place the electrolyte in an optical absorption cell with plane glass windows and to observe the progress of shaping the tip with a horizontally mounted optical microscope of 50 to 100 X. Tips that look perfectly shaped at this magnification are normally suitable for ion microscope work, although the actually effective area of the tip cap is often more than 10 times smaller than the resolution of this optical microscope.

PART V. DETERMINATION OF WORK FUNCTIONS FROM FIELD EVAPORATION DATA[1]

by E. W. Müller

Field evaporation of a high purity crystal produces the most perfect and clean metal surfaces that can presently be obtained by any experimental method. It is therefore of great interest to develop methods for measuring work functions of such ideally perfect surfaces. One way is to measure the field electron emission of these surfaces as is reported by Young and Müller.[2]

The problem to be considered now is if field evaporation data alone could not be used for measuring work functions. As was shown in 1956 field evaporation[3] can be described as the evaporation of the metal ion over the potential hump that is determined by the external field and the image force. The evaporation field is

$$F = e^{-3} (\Lambda + V_I - \varphi - kT \ln t/t_0)^2, \qquad (1)$$

and as the heat of vaporization from the repeatable step at the kink of a net plane edge is the same all over the crystal, one obtains an equation between φ and F. The absolute determination of F cannot be done with accuracy, but one may measure the ratio of the field strengths at two different crystal planes by using the fact that for a given tip radius the best image field for ion emission is quite well defined, and the best image voltage can be reproduced to about 1%. By assuming a certain value of φ for one crystal plane, the work function of another plane can be derived by setting the true evaporation field strengths inversely

proportional to the respective best image voltages. This method was described briefly in Acta. Met. (1958),[4] but no more measurements have been made since then.

A better method which is applicable to the determination of φ for one plane seems to be the performance of two evaporation measurements in which the value of the last term in Eq. (1) is varied; this way one obtains two equations for the two unknowns, F and φ.

It can be foreseen that these measurements will have to be quite accurate, as the last term in Eq. (1) is less than 1 ev at room temperature, and much smaller at the more desirable lower temperatures. This compares unfavorably with the 5 to 10 ev terms of the rest of the equation.

The last term can be varied in two different ways, either by making the two evaporation experiments with different times t, or by doing it at different temperatures T. The first way seems to be not too good as all the variation which can practically be achieved is a factor of two, when one makes one evaporation with a precisely to be measured voltage pulse of 10^{-5} seconds, and the other one during 100 sec. Therefore only one exploratory experiment was made in order to see if the pulse evaporation gives indeed a different field evaporation end form compared to a long time field evaporation. To that purpose the peak amplitude of 10^{-2} seconds pulses was slowly raised so that the field evaporation end form for this short evaporation time was reached. In a two color combination photo, which cannot be reproduced here, this represents the first, red image. Then the tip was field evaporated again by

very slowly raising the dc high voltage, until a few atoms had
disappeared within about one minute. The picture then obtained
is the green one in the color print. The combination photo shows
clearly that starting from the pulse end form the slow field
evaporation begins at the rim of the 011 plane and along the
[110]-zones. This should be so if Eq. (1) is valid and the color
marked regions are of higher work function. This experiment could
have been extended by further increasing the dc evaporation field
and comparing the next pair of photographs. This way a map of
the relative work function distribution could be displayed. The
important feature is that each time so few atoms are removed, that
the over all field distribution on the tip is not noticeably changed.

A more promising way to get this map of work function distribu-
tion and eventually, the absolute work function, is to field
evaporate at different temperatures. Here one can vary the last
term of Eq. (1) from 60 mevto .9 ev when one goes from liquid
hydrogen temperature to room temperature. In these experiments
it is probably more practical to establish the field evaporation
end form at the high temperature T_2 by applying the voltage V_2.
Then the tip is cooled to liquid hydrogen temperature T_1 and the
high temperature end form photographed with perfect resolution.
Now field evaporation will be continued at temperature T, each
time applying the voltage V, for a given time t (mostly 60 sec).
In a series of color photographs the progress of field evaporation
as the high temperature end form is gradually changing into the
low temperature end form has been illustrated. This time the atoms
are removed first at the low work function regions. Numerical values

of work functions can in principle be calculated from the ratio of V_{21}/V_T, which one obtains when Eq. (1) is written down for two different temperatures and φ is expressed as a function of V_{21}/V_T:

$$F_1 = \beta\, V_1 \qquad\qquad F_2 = \beta\, V_2 \tag{2}$$

$$\frac{F_1}{F_2} = \frac{V_1}{V_2} = \frac{(\Lambda + V_1 - \varphi - k\,T_1\, \ell n\ t/t_0)^2}{(\Lambda + V_1 - \varphi - k\,T_2\, \ell n\ t/t_0)^2} \tag{3}$$

$$\varphi = \Lambda + V_I - k\,T, \ \ \ell n\ t/t_0\ \frac{T_2/T_1\,\sqrt{V_1/V_2} - 1}{\sqrt{V_1 V_2} - 1}\ . \tag{4}$$

To illustrate the sensitivity of the method the voltage ratio as a function of T with φ as a parameter was plotted in Fig. 1. One sees that the tip temperature has to be determined rather accurately, and the high voltage must be kept quite constant and should be read to better than .1 of one per cent.

So far reliable quantitative measurements have not yet been made. The color slides mentioned above were obtained with the conventional ground joint FIM. As the high field was always kept on, there was no surface contamination. A charcoal trap and a titanium getter prevented water and nitrogen etch when the tip was at higher temperatures. The work function data obtained for the various crystal planes on tungsten give a much wider range than was expected from earlier measurements,[6] about 4 ev for the (116) plane to 6.8 ev for the vicinity of (011). The main objection to be made is that field evaporation in this series of measurements was don in the presence of about 1 micron of He as the imaging gas. This causes the arrival of electrons of several hundred volt energy

Fig. I
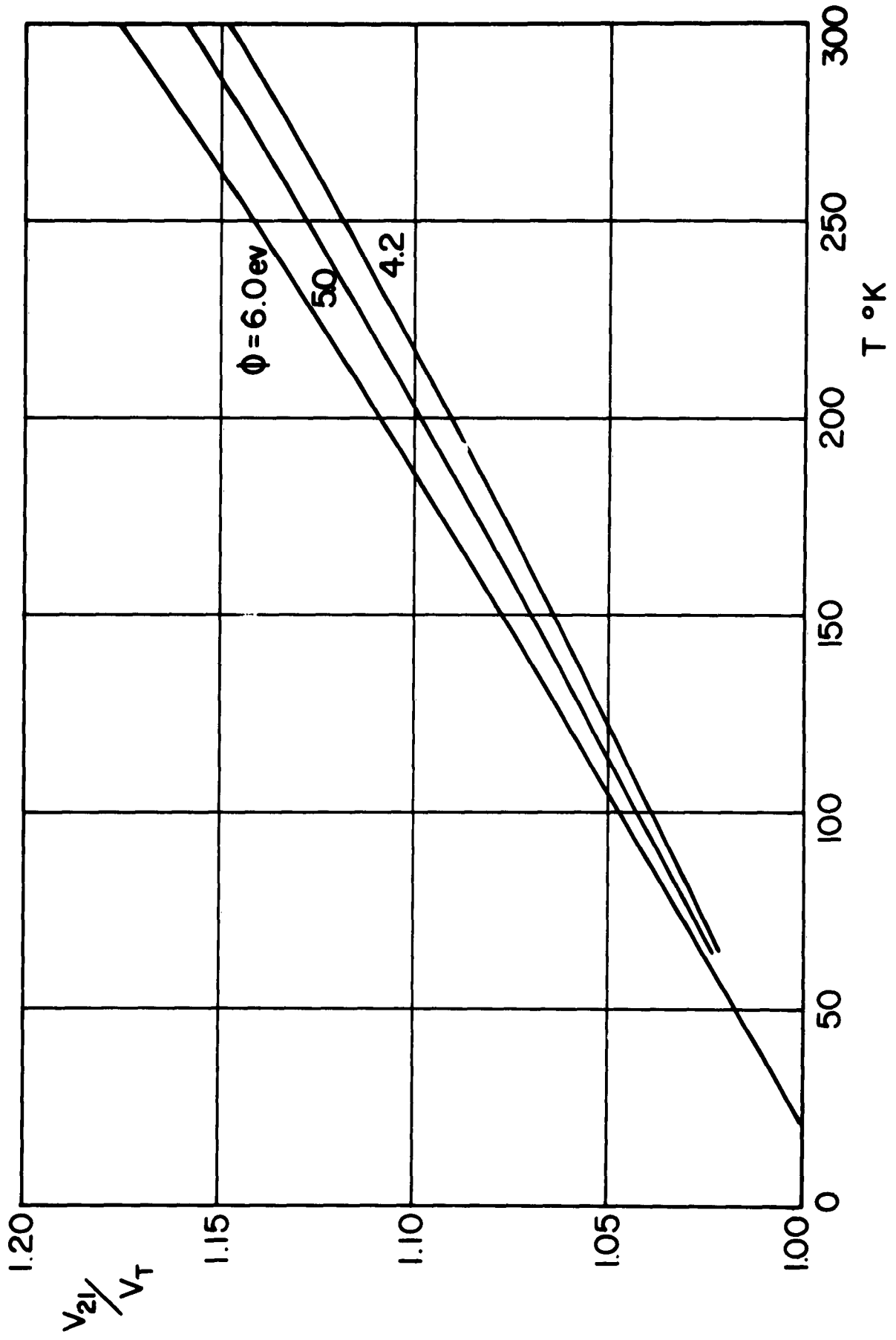
at the surface from ionization in space during the evaporation process. As R. D. Young has suggested[5] the electrons may transfer a sufficiently large fraction of their energy to surface metal atoms and bring them over the hump at a slightly lower field than would be required for field evaporation in high vacuum.

Recent experiments were then made in a baked FIM of the variety used at the beginning of field ion microscopy which have a double dewar mantle around the cold finger that carries the tip. The high tip temperature from the primary evaporation was maintained by putting an alcohol bath of exactly 200^0K into the cold finger and the surrounding dewar and by also immersing the screen into a cold bath, so that the tip was in thermal equilibrium. Evaporation was always done in high vacuum, and clean He gas for imaging was each time filled by diffusion through heated vycor glass. Low work function areas were mapped again with the color printing technique. Compared to the results obtained by evaporation in gas one finds that now the 111 vicinity has the lowest φ, followed by the vicinity of 001, and then by 111 itself. Quantitatively the data fitted not very well, as the voltage ratio was in the region of 1.05 to 1.06 rather than the expected value of 1.09 to 1.12.

All these recent measurements are reported with some reservation, as more data have to be collected to see how reproducible they are. One will then be in a position to test the validity of the original assumption of the simple field evaporation formula of Eq. (1). After all, the use of the image force concept at these extremely high fields is of course questionable. The polarization term $\frac{\alpha_i}{2} F^2$

containing the unknown polarizability of the metal ion might have to be included into the vaporization energy. One may also have to consider the zero point energy of the surface atoms and possibly also tunneling.

If all these possible corrections turn out to be either small or can be taken into account, the described method for the determination of work functions from absolutely perfect crystal surfaces by an entirely new method using electron acceptance rather than emission will be valuable. If the corrections are large, then the understanding of the mechanism of field evaporation will be advanced.

BIBLIOGRAPHY

1. E. W. Müller, presented at Field Emission Symposium, Williamstown, August 1961.

2. R. D. Young and E. W. Müller, J. Appl. Phys. 33, January 1962.

3. E. W. Müller, Phys. Rev. 102, 618 (1956).

4. E. W. Müller, Acta. Met. 6, 620 (1958).

5. R. D. Young, Field Emission Symposium, McMinnville, August 1960.

6. E. W. Müller, J. Appl. Phys. 26, 732 (1955).

DISTIRBUTION LIST

Agency	Number of Copies
Air Force Office of Scientific Research ATTN: Solid State Sciences Division Washington 25, D.C.	3
Air Force Office of Scientific Research ATTN: Technical Library (SRGL) Washington 25, D.C.	2
ASTIA (TIPCR) Arlington Hall Station Arlington 12, Va.	10
ARDC (RDRS) Andrews AFB Washington 25, D.C.	1
EOAFRD ARDC 47 Cantersteen Brussels, Belgium	1
HQ USAF (AFDRT) Washington 25, D.C.	1
ARL (Technical Library) Bldg. 450 Wright-Patterson AFB, Ohio	1
WADD (WWAD) Wright-Patterson AFB, Ohio	1
WADD (Metals and Ceramics Lab) Materials Central Wright-Patterson AFB, Ohio	1
WADD (Physics Lab) Materials Central Wright-Patterson AFB, Ohio	1
WADD (Materials Information Branch) Materials Central Wright-Patterson AFB, Ohio	1
Institute of Technology (AU) Library MCLI-LIB, Bldg. 125, Area B Wright-Patterson AFB, Ohio	1
ARL (Metallurgy) AFRD Wright-Patterson AFB, Ohio	1

Agency	Number of Copies
ARL (Physics, Solid State) AFRD Wright-Patterson AFB, Ohio	1
AFOSR (SRLTL) Holloman AFB, New Mexico	1
AFCRL (CRRELA) Laurence G. Hanscom Field Bedford, Massachusetts	1
AFFTC (FTCTL) Edwards AFB, California	1
AEDC (AEOIM) Arnold Air Force Station, Tennessee	1
AFSWC (SWOI) Kirtland AFB, New Mexico	1
Commander Army Rocket and Guided Missile Agency ATTN: ORDXR-OTL Redstone Arsenal, Alabama	2
Office of the Chief of Research and Development Department of the Army ATTN: Scientific Information Washington 25, D.C.	1
Army Research Office (Durham) ATTN: CRD-AA-IP Box CM, Duke Station Durham, North Carolina	1
Commanding Officer Ordnance Materials Research Office (ATTN: PS C Div.) Watertown Arsenal Watertown 72, Massachusetts	1
Commanding Officer Watertown Arsenal ATTN: Watertown Arsenal Labs, Tech. Reports Section Watertown 72, Massachusetts	1
Commander Signal Corps Engineering Laboratory ATTN: SIGFM/EL-RPO Fort Monmouth, New Jersey	1

Agency	Number of Copies
Director U.S. Naval Research Laboratory ATTN: Library Washington 25, D.C.	1
Department of the Navy Office of Naval Research ATTN: Code 423 ATTN: Code 421 Washington 25, D.C.	2
Officer in Charge Office of Naval Research Navy No. 100 Fleet Post Office New York, New York	1
Commanding Officer Naval Radiological Defense Laboratory San Francisco Naval Shipyard San Francisco 24, California	1
Dr. D. F. Bleil Associate Technical Director for Research U.S. Naval Ordnance Lab White Oak, Silver Spring, Maryland	1
National Aeronautics and Space Agency ATTN: Library 1520 H St., N. W. Washington 25, D.C.	1
Ames Research Center (NASA) ATTN: Tech Library Moffett Field, California	1
High Speed Flight Station (NASA) ATTN: Tech Library Edwards AFB, California	1
Langley Research Center (NASA) ATTN: Tech Library Langley AFB, Virginia	1
Lewis Research Center (NASA) ATTN: Tech Library 21000 Brookpark Road Cleveland 35, Ohio	1

Agency	Number of Copies
Wallops Station (NASA) ATTN: Tech Library Wallops Island, Virginia	1
Division of Research U.S. Atomic Energy Commission Division Office Washington 25, D.C.	1
U.S. Atomic Energy Commission Library Branch Tech Information Div., ORE P. O. Box No. E Oak Ridge, Tennessee	1
Major John Radcliffe ANP Office U.S. Atomic Energy Commission Washington 25, D.C.	1
Oak Ridge National Laboratory ATTN: Central Files Post Office Box P Oak Ridge, Tennessee	1
Brookhaven National Laboratory ATTN: Research Laboratory Upton, Long Island, New York	1
Argonne National Laboratory ATTN: Librarian 9700 South Cass Avenue Argonne, Illinois	1
Document Custodian Los Alamos Scientific Laboratory P. O. Box 1663 Los Alamos, New Mexico	1
Ames Laboratory Iowa State College P. O. Box 14A, Station A Ames, Iowa	1
Knolls Atomic Power Laboratory ATTN: Document Librarian P. O. Box 1072 Schenectady, New York	1

Agency	Number of Copies
National Science Foundation 1901 Constitution Avenue, N. W. Washington 25, D.C.	1
National Bureau of Standards Library Room 203, Northwest Building Washington 25, D.C.	1
Director Office of Technical Services Department of Commerce Technical Reports Branch Washington 25, D.C.	1
Chairman Canadian Joint Staff (DRB/DSIS) 2450 Massachusetts Avenue, N. W. Washington, D.C.	1
Defense Research Member Canadian Joint Staff ATTN. Mr. H. C. Oatway Director of Engineering Research Defense Research Board Ottawa, Canada	1
Institute of the Aeronautical Sciences ATTN: Librarian 2 East 64th Street New York 21, New York	1
RAND Corporation 1700 Main Street Santa Monica, California	2
Semiconductor-Components Library Texas Instruments, Inc. P. O. Box 5012 Dallas 22, Texas	1